

1 **Title**

2 Contrasting a reference cranberry genome to a crop wild relative provides insights into
3 adaptation, domestication, and breeding

4 **Running title**

5 Domestication of the cranberry genome

6 **Authors**

7 Joseph Kawash², Kelly Colt¹, Nolan T. Hartwick¹, Bradley W. Abramson¹, Nicholi Vorsa^{3,4}, James
8 J. Polashock², Todd P. Michael¹

9 **Affiliations**

10 ¹Plant Molecular and Cellular Biology, Salk Institute of Biological Sciences, La Jolla, California
11 92037, USA

12 ²USDA, Agricultural Research Service, Genetic Improvement of Fruits and Vegetables Lab,
13 125A Lake Oswego Rd., Chatsworth, New Jersey 08019, USA

14 ³P.E. Marucci Center for Blueberry and Cranberry Research, 125A Lake Oswego Rd.,
15 Chatsworth, New Jersey 08019, USA.

16 ⁴Department of Plant Biology and Pathology, Rutgers University, 59 Dudley Rd., New
17 Brunswick, NJ 08901, USA

18

19 **Corresponding authors:**

20 Todd P. Michael, tmichael@salk.edu
21 James Polashock, james.polashock@usda.gov

22

23 **Author ORCID**

24 JK: 0000-0003-4168-1319

25 KC: 0000-0001-8913-4678

26 NTH: 0000-0001-7916-7791

27 BWA: 0000-0003-0888-3648

28 NV: 0000-0002-7976-3486

29 JP: 0000-0002-7977-2921

30 TPM: 0000-0001-6272-2875

31

32

33

34

35 Abstract

36 Cranberry (*Vaccinium macrocarpon*) is a member of the Heath family (Ericaceae) and is a
37 temperate low-growing woody perennial native to North America that is both economically
38 important and has significant health benefits. While some native varieties are still grown today,
39 breeding programs over the past 50 years have made significant contributions to improving
40 disease resistance, fruit quality and yield. An initial genome sequence of an inbred line of the
41 wild selection ‘Ben Lear,’ which is parent to multiple breeding programs, provided insight into the
42 gene repertoire as well as a platform for molecular breeding. Recent breeding efforts have
43 focused on leveraging the circumboreal *V. oxycoccus*, which forms interspecific hybrids with *V.*
44 *macrocarpon*, offering to bring in novel fruit chemistry and other desirable traits. Here we
45 present an updated, chromosome-resolved *V. macrocarpon* reference genome, and compare it
46 to a high-quality draft genome of *V. oxycoccus*. Leveraging the chromosome resolved cranberry
47 reference genome, we confirmed that the Ericaceae has undergone two whole genome
48 duplications that are shared with blueberry and rhododendron. Leveraging resequencing data
49 for ‘Ben Lear’ inbred lines, as well as several wild and elite selections, we identified common
50 regions that are targets of improvement. These same syntenic regions in *V. oxycoccus*, were
51 identified and represent environmental response and plant architecture genes. These data
52 provide insight into early genomic selection in the domestication of a native North American
53 berry crop.

54 Introduction

55 The American or large-fruited cranberry, *Vaccinium macrocarpon*, is one of only three cultivated
56 fruit species that are native to North America. The tart fruit is valued for its many human health
57 benefits when consumed. For example, cranberry fruit is high in antioxidants, helps prevent
58 urinary tract infections, has anti-atherogenic effects, and helps prevent dental caries [1–6]. The
59 U.S. is the leading producer of cranberries with production of over 359,000 metric tons in 2019.
60 The total value of the U.S. cranberry production in 2019 was \$224.8 million dollars [7]. Canada
61 and Chile are also major producers of cranberries with annual production in 2018 of about
62 195,000 and 106,000 metric tons, respectively [8] with minor production in other parts of the
63 world. The most important products marketed are sweetened-dried-cranberries (SDCs) and
64 juice products.

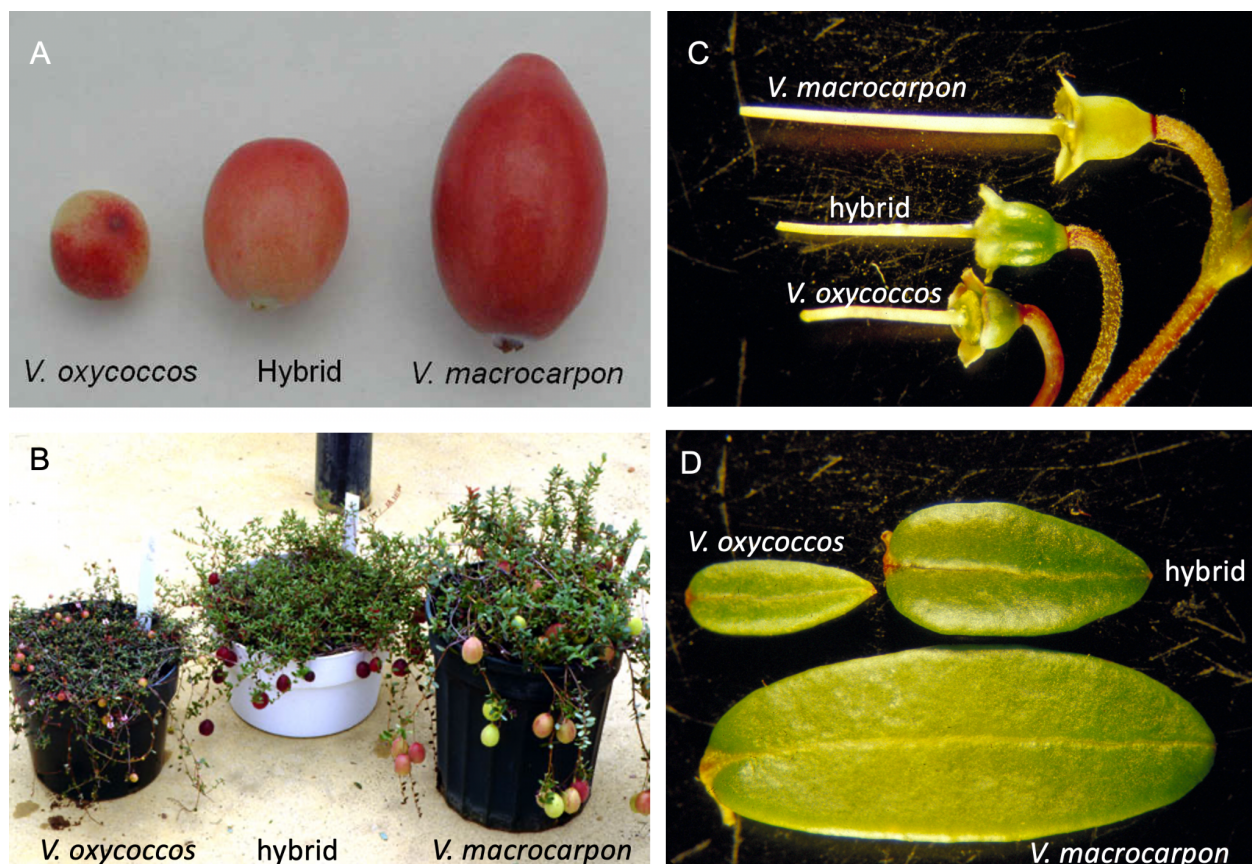
65 *Vaccinium macrocarpon* is a member of the Heath family (Ericaceae). Although
66 wetland-adapted, cranberries are low-growing woody perennial vines typically growing in
67 well-drained low pH (<5.5) sandy soils that are also low in nutrients. The roots lack root hairs
68 and are colonized with Ericoid mycorrhizae that aid in nutrient uptake [9]. The vines produce
69 stolons that root at various points, forming solid mats of vegetation, and cultivars are clonally
70 propagated from cuttings. The leaves are simple and ovate with blades that measure 5-17 mm
71 in length and 2-8 mm wide [10]. *V. macrocarpon* is diploid ($2n = 2x = 24$) and self-fertile [10].
72 Vertical shoots called ‘uprights’ bear the flowers and developing fruit. Cranberry blooms in early
73 summer and each upright typically bears 5-7 white to pinkish hermaphroditic protandrous
74 flowers (Figure S1). The flowers are 4-merous with eight anthers and an inferior ovary. The
75 inflorescence is semi-determinate, with the flowering shoot resuming vegetative growth

76 post-flowering. The size and number of fruit that develop per upright vary depending on the
77 cultivar and pollination efficiency. Most modern cultivars have an average mature fruit weight of
78 about 1.5-2.5 grams. There are four air-filled locules in the mature fruit, allowing them to float
79 during water harvesting. Like most temperate woody perennials, cranberries go through a winter
80 dormancy period and require 1,000-2,500 hours of chilling to resume growth and bloom in the
81 spring [11,12].

82 The small-fruited cranberry, *V. oxycoccus*, is similar to *V. macrocarpon* in many ways (Figure 1).
83 It has a similar growth habit (low-growing perennial woody vines) and it thrives in similar soils
84 and habitats as *V. macrocarpon*. *V. oxycoccus*, has limited commercial production in Russia,
85 Estonia, and Lithuania, but is mostly harvested from the wild. The ripe berries are usually red
86 and contain similar classes of phytochemicals (e.g. anthocyanins, proanthocyanidins, flavonols,
87 etc.) as the large-fruited cranberries. Fruit size is variable, but smaller (0.6 – 1.2 cm) than *V.*
88 *macrocarpon*. The native range of *V. oxycoccus* is circumboreal, including northern Europe,
89 northern Asia and northern North America (Figure S1). One of the key differences is in ploidy
90 level. As noted above, *V. macrocarpon* is diploid, while *V. oxycoccus* occurs as diploid ($2n = 2x$
91 = 24), tetraploid ($2n = 48$) and hexaploid ($2n = 72$) levels [13]. Diploid *V. oxycoccus* occurs only
92 above the 51st parallel except at high elevation, such as the Columbia mountain range [14].
93 Isozyme and recent sequence-based data suggest the North American diploid and tetraploid *V.*
94 *oxycoccus* are likely different species [15,16]. How the hexaploids fit into the overall taxonomy is
95 still under debate. The leaves of *V. oxycoccus* are generally smaller (8– 10mm long and 1–
96 2.5mm wide) than those of large-fruited cranberry, but length varies depending on ploidy level.
97 The leaves of the diploid representatives, that are the subject of this paper, are about 3– 5mm
98 long and 1– 2mm wide. Flowering is determinate and this species does not produce flowering
99 uprights. Rather, the flowers arise from the stolons and tend to be darker pink than those of *V.*
100 *macrocarpon*.

101

102



103 **Figure 1. *Vaccinium macrocarpon* (Vmac) and *Vaccinium oxycoccus* (Voxy) are
104 interfertile and have distinct morphology.** A) Fruit, B) plants, C) pistils (attached to pedicels),
105 and D) leaves from Vmac, Voxy and the interspecific F1 hybrid.

106 Breeding of large-fruited cranberry is in its infancy relative to most other crops, with commercial
107 cultivars removed only one to three generations from the wild. In fact, some varieties grown
108 today are still wild selections. The first breeding program was started in 1929 by the USDA in
109 response to an outbreak of false blossom, a phytoplasma-incited disease. The first varieties
110 developed in this program that were considered more 'resistant' to the phytoplasma (less
111 preferable in feeding studies to the leafhopper vector of the disease) were released between
112 1950-1961. One of those varieties, 'Stevens,' is still one of the most widely grown cultivars.
113 Breeding programs in New Jersey and Wisconsin, as well as a few private companies, are
114 releasing new varieties with superior attributes, such as increased yield and uniform fruit color.
115 Thirteen new varieties were released between 1994 and 2017. One focus area, particularly in
116 the New Jersey breeding program, is fruit rot resistance. Still, all cranberry breeding to date has
117 been limited to a single species, *V. macrocarpon*.

118 It is likely that in the wild, cranberries went through a genetic bottleneck during the ice age,
119 potentially limiting variation in the available germplasm [17]. Thus, interspecific hybridization
120 offers the opportunity to expand the gene pool. *V. oxycoccus* is also reported to be very high in
121 antioxidants and bioactive compounds, some of which may be more bioavailable than those
122 found in *V. macrocarpon* [18]. Although there is some overlap in native range, *V. oxycoccus* is
123 adapted to more northern latitudes, e.g., north of the 51st parallel, and may be more cold

124 tolerant than *V. macrocarpon* (Figure S1). In addition, *V. oxycoccus*, being circumboreal,
125 responses to photoperiod are expected to differ as this species typically has a much shorter
126 growing season and day length varies with nearly 24 hours of light during summer. Finally, *V.*
127 *oxycoccus* may offer disease resistance genes that are not found in large-fruited cranberries.
128 Crop loss due to fruit rot remains one of the biggest challenges in the sustainable production of
129 cranberries.

130 We have successfully produced F1 interspecific hybrids between *V. macrocarpon* and diploid *V.*
131 *oxycoccus* and have a large F2 population segregating for many morphological, horticultural
132 and fruit chemistry traits. However, F1 hybrids exhibit lower gametophytic fertility, e.g., lower
133 pollen staining, than the parental species. As part of the ongoing breeding and genetics
134 program, we are interested in comparing the genomes of these two cranberry species. We
135 previously published a draft reference genome for the *V. macrocarpon* cultivar Ben Lear (BL)
136 that was very useful, yet still rather fragmented [19]. Recently, a genome for a second cultivar
137 Stevens (ST) and a fragmented assembly for *V. oxycoccus* was published [20]. Here we report
138 an updated chromosome scale assembly for the BL reference genome and an improved draft
139 genome of diploid *V. oxycoccus*. We further compared the genomes and transcriptomes of
140 these two species to begin documenting their similarities and differences, as we more
141 intensively use interspecific hybridization for domesticated cranberry improvement.

142 Results

143 Cranberry genome size

144 The first *Vaccinium macrocarpon* (Vmac) genome draft provided a resource for gene discovery
145 and marker development [19]. The initial draft was based on a fifth generation inbred of 'Ben
146 Lear' (BL-S5) and sequenced using Illumina short reads, resulting in an assembled genome
147 size of 420 Mb and a scaffold N50 length of 4,237 bp (Table 1). We endeavoured to improve
148 the draft genome, as well as sequence the undomesticated diploid *V. oxycoccus* (Voxy) with
149 which we can make interspecific hybrids (Figure 1). First, we estimated the genome size of the
150 Vmac, Voxy and the F1 hybrid (Vmac X Voxy) using k-mer frequency analysis based on short
151 read sequence [21]. The Vmac and Voxy genomes both had single k-mer frequency peaks
152 consistent with diploid and homozygous backgrounds with genome size estimates of 487 and
153 585 Mb respectively (Table 1; Figure S2; Table S1). The k-mer frequency genome size estimate
154 for Vmac is very close to the reported flow cytometry genome size estimate of 470 Mb [22].
155 Conversely, the F1 hybrid had a double peak, consistent with a hybrid of two genomes that have
156 distinct nucleotide compositions, suggesting there are distinct differences between the genomes
157 that can be exploited for applications such as breeding (Figure S2; Table S1).

158

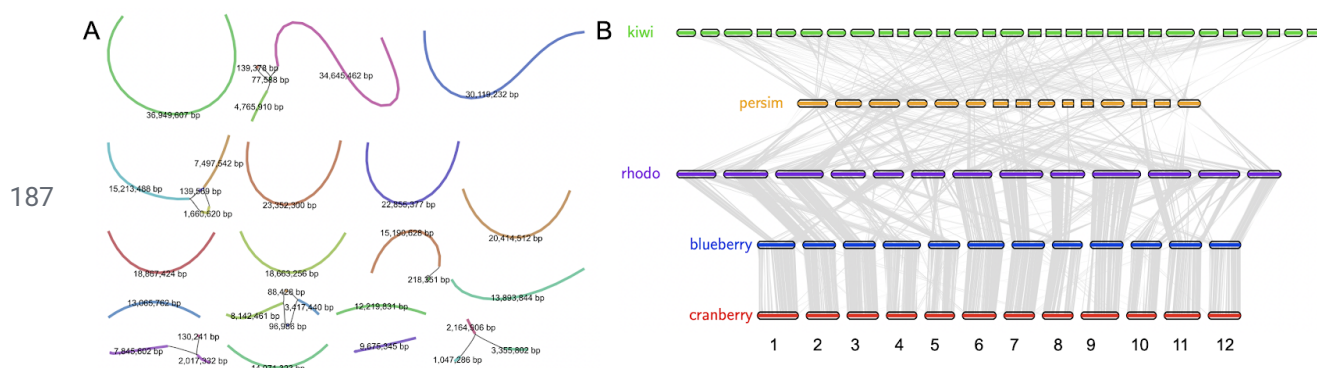
159 One indicator of interspecific compatibility is fertility of the offspring resulting from interspecific
160 crosses. Pollen in *Vaccinium* spp. is shed as a tetrad; four microgametophytes result from a
161 meiotic event held in a tetrahedron. Staining of the tetrads with lacto-phenol blue and counting
162 those pollen grains within each tetrad that take up the stain as potentially viable can be used as
163 an indicator of pollen viability. Pollen from 'Stevens' and other commercial cultivars was
164 estimated to be 99% viable, while accession NJ96-20 of Voxy was 56% and NJ96-127 of Voxy
165 was 80%. This shows that there is some pollen infertility in this limited representation of Voxy.

166 The F1 hybrids varied from about 29%-53% pollen stainability. This suggests at least some
167 interspecific meiotic recombination leads to interlocus allelic instability in the gametophytic
168 generation in the F1 (Vmac x Voxy) hybrids.
169

170 *Updated V. macrocarpon (Vmac) genome*

171 Long read sequencing has enabled a new wave of near-complete plant genomes [23]. We
172 sequenced the same fifth generation inbred (BL-S5) using Oxford Nanopore Technologies
173 (ONT) long read sequencing, and assembled the reads using a correction-free overlap, layout,
174 consensus (OLC) strategy [24]. The resulting genome was an extremely contiguous assembly
175 with a total length of 484 Mb in 124 contigs and a 15 Mb N50 length, representing whole
176 chromosome arms with few repeats in the genome assembly graph consistent with the inbred
177 nature of the line (Vmac_v1; Figure 2A;Table 1). The genome assembly was collinear with the
178 chromosome-scale, haplotype-resolved blueberry (*Vaccinium corymbosum*) genome (Figure
179 S3) [25]. We scaffolded the Vmac_v1 genome into chromosomes leveraging the high contiguity
180 of the chromosomes and the synteny with haplotype1 of blueberry, and then validated the order
181 and orientation of the Vmac scaffolds (chromosomes) reported here using high-density genetic
182 map markers [26]. The resulting Vmac chromosome-scale assembly was contiguous with other
183 closely related species that have chromosome-scale assemblies such as rhododendron
184 (*Rhododendron williamsianum*) [27], persimmon (*Diospyros lotus*) [28], tea (*Camellia sinensis*)
185 [29] and kiwi (*Actinidia chinensis*) [30] (Figure 2B).

186



187
188 **Figure 2. Chromosome scale assembly of *Vaccinium macrocarpon* (Vmac).** A) Genome
189 assembly graph of the cranberry genome resulted in chromosome scale, reference quality,
190 contigs and very few “hairballs” (graph bubbles, or multiple connections due to heterozygosity
191 and repeats). Contig size (bp) labeled, and color is randomly assigned. B) Protein based
192 alignment of the cranberry (red; *Vaccinium macrocarpon*) genome with blueberry (blue;
193 *Vaccinium corymbosum*), rhododendron (purple; rhodo; *Rhododendron williamsianum*),
194 persimmon (orange; persim; *Diospyros lotus*), and kiwi (green; *Actinidia chinensis*). Lines (grey)
195 symbolize pairwise syntetic blocks between genomes.
196

197 *The V. oxycoccus (Voxy) genome*

198 Next, we sequenced the diploid Voxy genome using the same long read approach as with
199 Vmac. Unlike Vmac, Voxy did not assemble into chromosome arms, yet was of high quality with

200 a total length of 484 Mb in 1,692 contigs with an N50 length of 1.8 Mb (Table 1; Figure S4). The
201 more fragmented nature of the Voxy assembly most likely reflects the underlying heterozygosity
202 relative to the near-homozygous Vmac fifth-generation inbred (BL-S5). Both Vmac and Voxy
203 assemblies were very complete with 95 and 94 BUSCO percentages, respectively (Table 1;
204 Table S2). Repeat annotation that leveraged a *de novo* pipeline [31], predicted that 44.8 and
205 43.9% of the Vmac and Voxy genomes were repeat sequences, respectively (Table 1; Table
206 S3). We generated full-length cDNA sequences using the ONT platform and used these reads
207 to predict protein coding genes in Vmac and Voxy and found 48,647 and 50,621 respectively
208 (Table 1). We annotated the telomeres (AAACCCT), which revealed Vmac has longer telomeres
209 (~12 kb) than Arabidopsis (~3 kb) [32] (Figure S5). In addition, we found centromeres with
210 higher order repeats and base arrays of 124 bp (Figure S5).

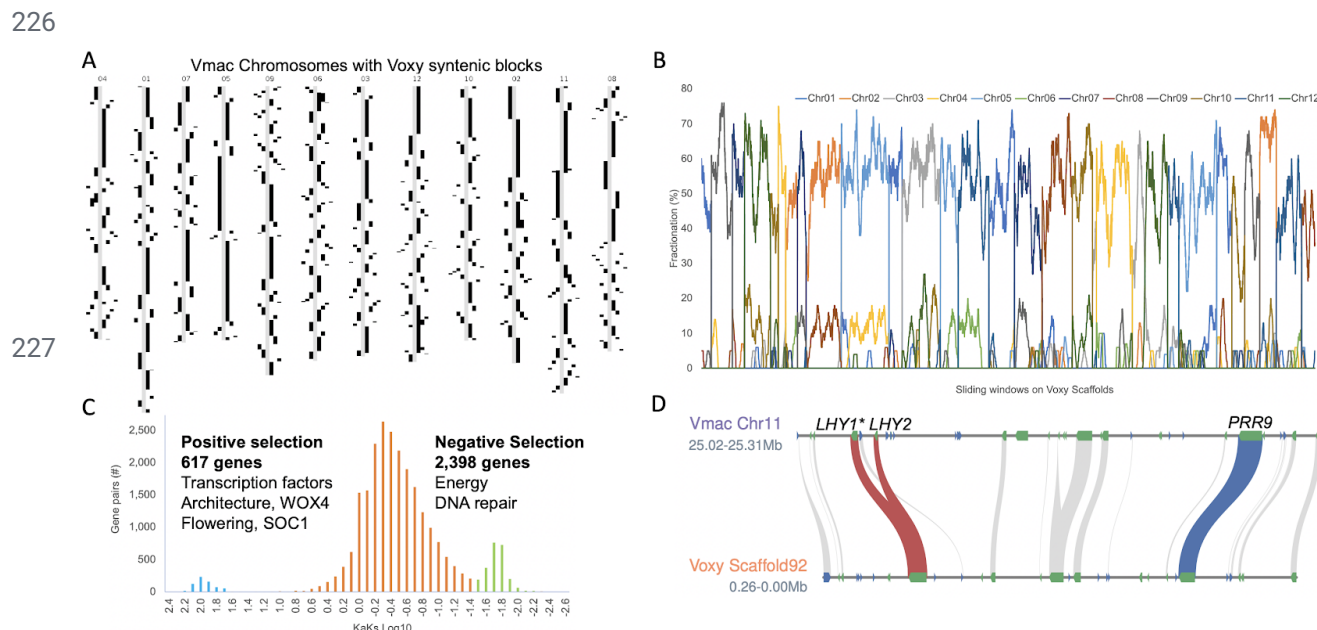
211

Table 1. Cranberry genome assembly statistics.

	Vmac_v1 (Draft_2014)	Vmac	Voxy
	CNJ99-125-1	CNJ99-125-1	NJ96-20
Estimated genome size Kmer19 (Mb)	487	487	585
Estimated genome size flow cytometry (Mb)	470	470	NA
Assembled genome size (Mb)	420	484	484
Contig (#)	231,033	124	1,692
Contig N50 length (bp)	4,214	15,310,187	1,785,328
Scaffold (#)	229,745	13	NA
Scaffold N50 length (bp)	4,237	39,611,093	NA
BUSCO	85	95	94
Repeat content (%)	39.5	44.8	43.9
Predicted genes (#)	36,364	48,647	50,621
Anchor Coverage (%)	NA	71	71
Anchors > 1kb	NA	30,112	30,090
Genome Block Coverage (%)	NA	93	94
Genome Block Coverage Duplicated (%)	NA	4	4
Genes within Block (%)	NA	67	69
Blocks > 100kb	NA	412	412
NA, not available			

212

213 The genomes of Vmac and Voxy are highly syntentic, with 80% of the genomes contained in
214 syntetic blocks (Figure 3A; Table 1; Figure S6). Highly conserved syntetic gene connections
215 are maintained between Vmac and Voxy, such as the tight linkage between the core circadian
216 clock genes *LONG ELONGATED HYPOCOTYL 1 (LHY)* and *PSEUDO RESPONSE*
217 *REGULATOR 9 (PRR9)* that dates back to mosses (Figure 3D). Vmac does have a tandem
218 duplication of *LHY* that is specific to Vmac. It is not found in Voxy or blueberry (Figure S7).
219 Within the syntetic blocks, there is 60% fractionation (4/10 genes are lost between Vmac and
220 Voxy) and remnants of a previous whole genome duplication (WGDs) at 10% fractionation
221 (Figure 3B). While both Vmac and Voxy maintain 5% of their genomes in 2 syntetic blocks
222 (Figure S6), there are 54 and 70 genes that are specifically duplicated between them
223 respectively (and retained in both). Voxy genes retained in duplicate are overrepresented for
224 phenolic glucoside malonyltransferase that is involved with pest defense [33], providing a
225 possible source of genes for Vmac improvement.
226



228 **Figure 3. *V. macrocarpon* is highly syntentic to its wild relative *V. oxycoccos*.** A) Voxy
229 syntetic blocks (black) visualized on Vmac (grey) chromosomes. B) Fractionation of Vmac
230 genes (chromosomes labeled in color) across Voxy scaffolds shows 2:2 syntetic depth with
231 60% genes present in the most recent whole genome duplication (WGD). C) Non-synonymous
232 (Ka) by synonymous (Ks) base changes between Vmac and Voxy syntetic pairs reveals genes
233 under positive (blue; far left) and negative (green; far right) selection. D) Conserved linkage
234 between core circadian clock genes *LATE ELONGATED HYPOCOTYL (LHY)* (red lines) and
235 *PSEUDO RESPONSE REGULATOR 9 (PRR9)* (blue line) maintained on Vmac Chr11 and Voxy
236 Scaffold92; other syntetic genes in the region (grey). Vmac has a tandem duplication of LHY
237 (*LHY1* and *LHY2*) not found in Voxy, and under positive selection (*) in the cranberry cultivar
238 Mullica Queen (MQ).

239
240 Vmac and Voxy have different growth habits, architecture, flower and fruit sizes, as well as
241 distinct ecological ranges (Figure 1; Figure S1). We looked at the syntetic genes to determine

242 those under selective pressure between Vmac and Voxy and found that there were 617 genes
243 under positive selection ($Ka/Ks > 1$) and 2,398 under negative selection ($Ka/Ks < 1$) (Figure 3C;
244 Table S4). The genes under negative selection are related to primary processes such as energy
245 acquisition and DNA repair. In contrast, the genes under positive selection are transcription
246 factors, architecture genes (e.g. *WUSCHEL RELATED HOMEOBOX 4*, *WOX4*), and flowering
247 genes (e.g. *SUPPRESSOR OF OVEREXPRESSION OF CO 1*, *SOC1*) (Figure 3C; Table S4).
248 Tandem duplications (TDs) also provide clues as to the differences between closely related
249 species. Vmac and Voxy have 2,619 and 2,580 TD clusters, which is similar for other genomes
250 of this size range. While many of the TDs are shared between the two species, there are 37 and
251 41 unique GO terms that separate Vmac from Voxy respectively (Table S5,6). Vmac specific
252 TDs were focused on GO categories associated with plant architecture, lipid metabolism,
253 hormone stimulus, and phenol-containing compound metabolism. In contrast, Voxy unique TDs
254 were more focused on response to the environment (cold, wounding), toxin catabolic processes,
255 and root development (Figure S8).

256

257 Often crop wild relatives retain disease resistance genes that are lost in a crop during
258 domestication, resulting in the wild relatives having more or different disease resistance genes
259 [34]. Leveraging an approach that identifies genes with disease resistance domains [35], we
260 found that Voxy had 9,950 domains in 1,787 genes, while Vmac had 10,081 domains in 1,795
261 genes. 65% of the predicted disease resistance genes were shared between Vmac and Voxy in
262 syntenic blocks, which means 35% represent presence/absence variation (PAV) between the
263 two genomes (Table S7). Of the disease gene PAVs, 62 and 65% were in TD regions, consistent
264 with each species having amplification of disease resistance genes specific to their genomes
265 (Figure S9).

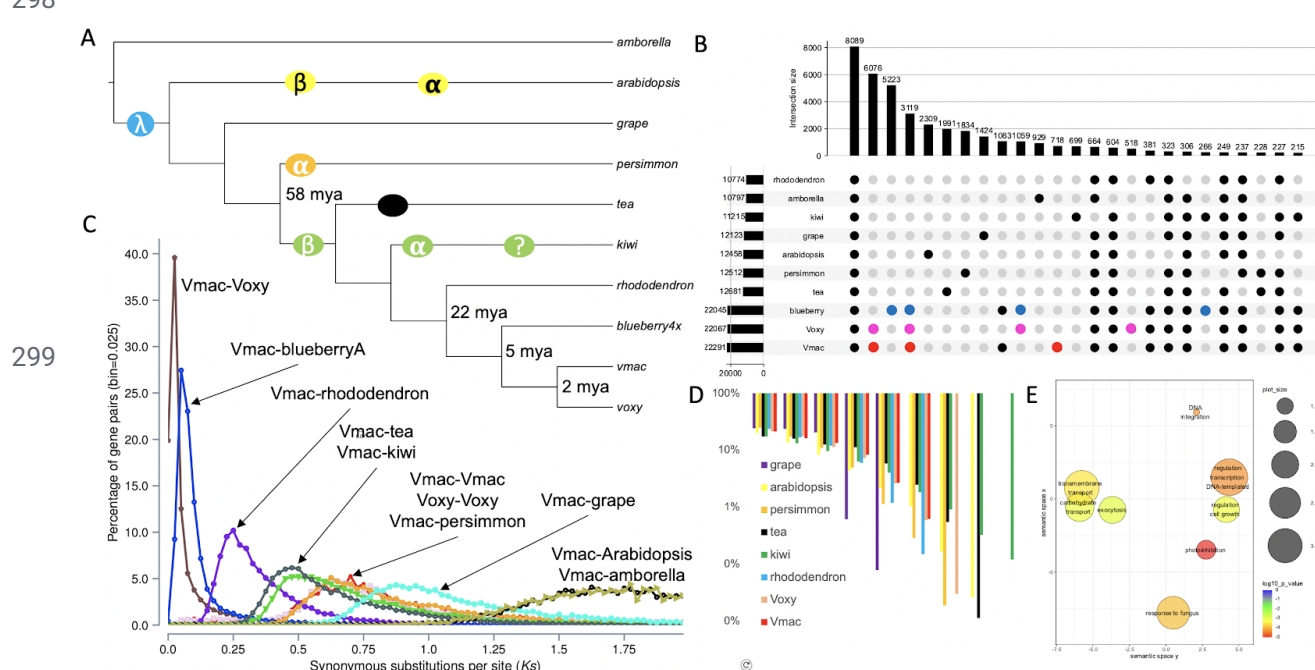
266

267 *Cranberry genome evolution*

268 Cranberry differs in specific ways from its close relative, highbush blueberry (*V. corymbosum*),
269 such as in stature (low-growing vine vs. crown-forming bush), fruit chemistry, and berry types
270 (e.g. ripe cranberries are firm, high in proanthocyanidins, high in acidity [36], and low in sugar (<
271 6%), while blueberries are soft and sweet (>12%). The contrast in fruit chemistry reflects
272 divergence in seed dispersal mechanism, i.e., abiotic (cranberries float on the water) versus
273 animal (blueberries are eaten by birds etc. that disperse the seeds). We clustered the
274 proteomes of Vmac, Voxy, blueberry, rhododendron, persimmon, tea, and kiwi to identify both
275 shared and cranberry-specific genes and pathways (Figure 4A). We found 8,089 orthogroups
276 (OGs) shared across all genomes, 6,076 specific to Vmac and Voxy, 5,223 specific to blueberry,
277 and 3,119 shared in the *Vaccinium* spp. (Figure 4B). There are fifteen overrepresented gene
278 ontology (GO) terms from cranberry specific orthogroups as compared to blueberry (Figure 4E;
279 Table S8). There were also 718 and 518 OGs specific to Vmac and Voxy respectively. The
280 overrepresented GO terms from these OGs in Voxy are pantothenate biosynthesis (vitamin B5)
281 and plant architecture; the latter being consistent with the genes under positive selection (Table
282 S4,8). In contrast, the overrepresented GO terms in Voxy were focused on nitrogen processes
283 (Table S8).

284

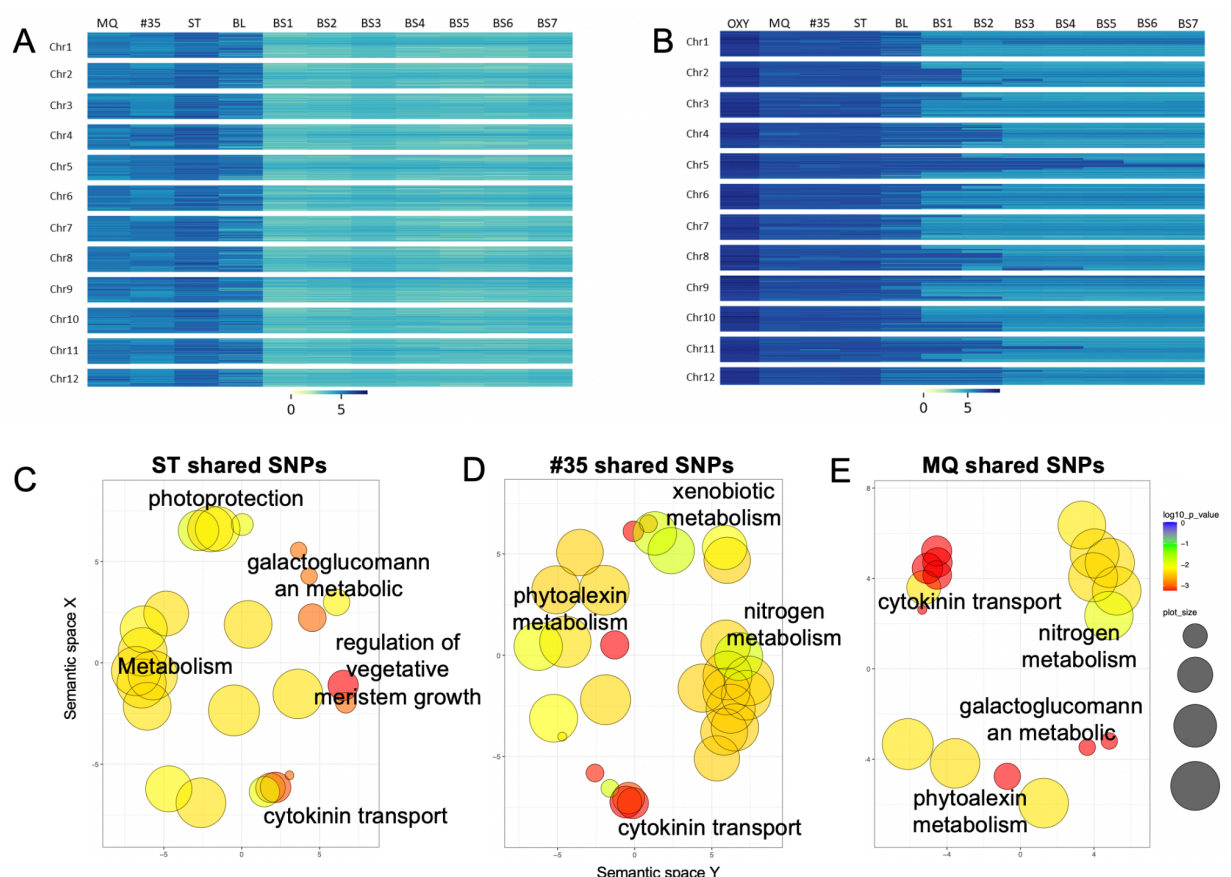
285 The chromosome-resolved Vmac genome provided the opportunity to gain a better
 286 understanding of the evolution of the cranberry genome. The recent chromosomal-scale
 287 assembly of rhododendron (*R. williamsianum*) suggested that there are two shared WGDs in the
 288 Ericales lineage [27] (Figure 4C). Consistent with Vmac containing these two WGD is the 4:1
 289 syntenic ortholog pattern between Vmac and amborella, which is the basal plant lineage without
 290 a WGD (Figure 4D). Based on synonymous substitutions (Ks) between syntenic ortholog pairs,
 291 Vmac is separated from its two closest relatives with chromosome-resolved genomes, blueberry
 292 and rhododendron, by 5 and 22 million years ago (mya) respectively. Moreover, while Vmac and
 293 Voxy diverged 1-2 mya, the Ks for its paralogous genes suggests the most recent WGD
 294 occurred 58 mya, which is consistent with the timing of the WGD found in kiwi (Ac- α) and
 295 rhododendron (Ad- β), but not persimmon (Figure 4A,C) that has its own WGD event (Dd- α)
 296 [27,37,38]. Therefore, Vmac and Voxy contained the two WGDs Ad- β and λ WGDs that have
 297 shaped their genomes.
 298



300 **Figure 4. Whole genome duplication evolution of cranberry.** A) Phylogenetic tree built with
 301 single copy proteins across amborella (*Amborella trichopoda*), arabidopsis (*Arabidopsis*
 302 *thaliana*), grape (*Vitis vinifera*), persimmon (*Diospyros lotus*), tea (*Camellia sinensis*), kiwi
 303 (*Actinidia chinensis*), rhododendron (*Rhododendron williamsianum*), blueberry 4x (tetraploid
 304 *Vaccinium corymbosum*), Vmac, and Voxy. Circles symbolize whole genome duplications
 305 (WGD) events; . B) Upset plot of the overlap between gene families. Red, pink and blue dots
 306 emphasize some of the similarities and differences among the *Vaccinium* spp. C) Synonymous
 307 substitution (Ks) distribution plot across species. D) Shared syntenic blocks compared to
 308 amborella across species. E) Significant gene ontology (GO) terms for cranberry (Vmac and
 309 Voxy) specific orthogroups (OGs) plotted in semantic space.
 310
 311 *Resequencing inbreds and parents reveal regions of selection*

312 Cranberry is a relatively young crop in terms of years post domestication, and many high value
313 cultivars are only modestly improved over wild selections [22]. We resequenced several
314 cultivars important to the cranberry breeding program to identify regions of the genome that may
315 still provide genetic resources for breeding as well as genes that are under selection in these
316 cultivars. We looked at four cultivars that represent three generations of breeding: Stevens (ST),
317 #35, Mullica Queen (MQ), and the Ben Lear (BL) parent. BL is a wild selection from 1901, while
318 ST and #35 are first generation selections from crosses of wild selections, and MQ is a second
319 generation offspring between a wild selection and #35 [26]. We also resequenced each
320 generation from the BL-Self series (BLS1-BLS7) to identify the variation that was lost during the
321 inbreeding process. We mapped the reads, identified SNPs between the cultivars and inbreds,
322 and then looked for trends in variation in 250 kb bins, which highlighted the regions of the Vmac
323 genome with high diversity (Figure 5A,B).

324



325

326 **Figure 5. Regions of high and low SNP diversity in a wild selection and breeding-derived**
327 **cranberry cultivars.** A) Unique SNPs identified in early ‘bred’ cultivars of cranberry (#35, MQ,
328 and ST) compared to the wild selection (BL) and a series of inbred lines (BS1-BS7) B) Shared
329 SNPs identified in early cultivated lines of cranberry (#35, MQ, and ST) compared to Voxy, the
330 wild selection (BL), and a series of inbred lines (BS1-BS7). Overrepresented GO terms from
331 shared SNPs across cranberry cultivars C) ST, D) #35 and D) MQ plotted in semantic space.
332

333 Voxy had the greatest SNP diversity, with over 99% of the 250 kb bins across the genome
334 containing a significant number of unique heterozygous SNPs. In fact, only two bins were found
335 to have a significantly lower number of unique heterozygous SNPs for Voxy. ST was the next
336 genotype to exhibit a relatively high amount of unique SNPs, with nearly 45% of the bins
337 containing a significantly large number of unique SNPs and only 7% of the bins being
338 significantly low in unique SNPs. The other Vmac cultivars had a reduced number of unique
339 SNPs. #35 had a high unique SNP count in 16% of the bins, and a low unique SNP count in
340 28% of the bins. MQ had a high unique SNP count in 11% of the bins and a low unique SNP
341 count in 31% of bins. BL had the lowest number of unique SNPs outside of the inbred line
342 (BL-S5) with only 4% of the bins containing a significantly high count of unique SNPs, and a low
343 unique SNP count in 79% of the bins across the genome. As expected, the 5th generation self
344 of Ben Lear (BL-S5) had a very low number of unique SNPs, with only a single bin having a
345 significantly high number of unique SNPs and over 99% of the bins being significantly devoid of
346 unique heterozygous SNPs (Figure 5A; Table S9).

347

348 These variable regions represent standing variation in wild populations as well as regions of
349 early domestication in this young crop. We next assessed the functional significance of these
350 highly variable regions by examining the GO terms of the underlying genes (Table S10-12). The
351 significant GO terms based on the genes in the variable regions of ST were related to plant
352 architecture, metabolism, and environmental response (Figure 5C; Table S10). In contrast, #35
353 and MQ both had significant GO terms related to terpene based phytoalexins (pest inhibitory
354 compounds), and nitrogen metabolism (Figure 5D,E; Table S11,12). #35 did have significant GO
355 terms in xenobiotic metabolism (metabolism of foreign chemicals) that was not found in either
356 ST or MQ, which must have been lost in the breeding and selection process leading to MQ.

357

358 Underlying these regions of higher variation, are genes that are under selection, representing
359 potential breeding targets. We looked at the selective pressure on the genes among the
360 cultivars to identify possible targets of improvement. We only found 18 genes under positive
361 selection ($Ka/Ks > 1$) between BL and ST consistent with these lines being either a wild selection
362 (BL) or a 1st-generation breeding selection (ST) (Table S13). In contrast, #35 and MQ had 785
363 and 786 genes under positive selection ($Ka/Ks > 2$) (Table S13), although there were no
364 significant ($P < 0.01$) GO terms associated with these genes. We looked at specific genes in
365 these lists for genes that have been the targets of selection. #35 and MQ share 34% (266)
366 genes under positive selection with genes associated with plant architecture and
367 photomorphogenesis: *EPIDERMAL PATTERNING FACTOR-like (EPFL)*, *SHOOT*
368 *GRAVITROPISM (SGR)*, *STEROL METHYLTRANSFERASE (SMT1)*, and *HEMERA (HMR)*.
369 Moreover, MQ had additional genes under positive selection in the photomorphogenesis,
370 flowering and circadian pathway: *LIGHT-DEPENDENT SHORT HYPOCOTYLS (LSH)*,
371 *ENHANCER OF AG-4 (HUA2)* and *LHY*. In addition to being under positive selection, *LHY* is
372 also tandemly duplicated in Vmac (Figure 3B), suggesting it may play an important role in the
373 domestication of cranberry consistent with the selection pressure on core circadian genes in
374 other crops [39].

375

376 **Discussion**

377 Here we describe an updated genome assembly for the highly inbred reference cranberry
378 accession Ben Lear (Vmac BL-S5) and a draft assembly for *V. oxycoccus* (Voxy) that is
379 currently being used in our cranberry improvement program. The chromosome resolved Vmac
380 genome confirmed the two WGD in the cranberry lineage that along with the more recent TDs
381 have acted to shape the domesticated cranberry genome. Moreover, comparison with Voxy and
382 more advanced selections of Vmac, revealed that response to the environment and plant
383 architecture are under selection. The Vmac reference genome and Voxy draft genome will
384 greatly facilitate current efforts to generate improved cranberry selections.

385

386 While we were preparing this manuscript a chromosome-resolved genome for a different
387 cranberry accession (Stevens; ST) and a fragmented Voxy genome assembly were published
388 [20]. It is exciting to see genomic resources emerge for this iconic North American crop and
389 surely having a high quality genome for a second accession will refine our knowledge of
390 cranberry biology. We compared our reference Vmac (BL-S5) genome assembly to the ST
391 assembly and found that the two two were highly collinear, but consistent with the lower contig
392 N50 length of the ST assembly, there is substantial telomere and repeat sequence missing
393 (Figure S10). This is evidenced by non-linear regions in the dotplot, higher rate of non-syntenic
394 orthologs and missing regions around the putative centromeres. A more thorough analysis of
395 these two genomes will be the focus of future work.

396

397 We reported previously that the sugars associated with the anthocyanins are distinct between
398 Vmac and Voxy [18]. Vmac contains primarily galactosides and arabinosides of the aglycones
399 cyanidin and peonidin, while Voxy contains mostly glucosides of the same aglycones. This
400 difference is important as it may affect antioxidant bioavailability. The sugar moiety is attached
401 to the anthocyanidin by specific UDP-glucose:flavonoid 3-O-glycosyltransferases (UF3GT).
402 Within the UF3GT is the highly conserved plant secondary product *glycosyltransferase* (PSPG)
403 box. Amino acids in the PSPG box are reported to determine sugar specificity [40]. Specifically,
404 the last amino acid in the PSPG box is reported to be specific for the sugar substrate with
405 histidine conferring specificity for galactose and glutamine conferring specificity for glucose [41].
406 We have identified two Anthocyanidin 3-O-glycosyltransferases that exist distinctly in Voxy and
407 Vmac (Vmac_055574 and Voxy_017508). The variant in Vmac contains histidine in the active
408 site (Chr11-43267493), consistent with the galactosides found in Vmac anthocyanins, while
409 Voxy has the glutamine amino acid associated with glucose specificity (Chr185-86547).
410 Interestingly F1 interspecific hybrids of Vmac x Voxy have intermediate anthocyanin glycoside
411 profiles, while about half the backcross (to Vmac) exhibit relatively high anthocyanin glucosides
412 [18]. We identified other anthocyanidin 3-O-glycosyltransferases within the genomes of both
413 Vmac and Voxy that may confer glycosylation of other flavonoids, e.g. flavonols conjugated to
414 galactosides and arabinosides. However, there is only one location in the Voxy genome that
415 contains the active site (which encodes the glutamine noted above), and only two in Vmac.
416 Although 2 active sites are identified in Vmac, only one (that encodes the histidine) active site is
417 located within a gene. Interestingly, just upstream of the annotated gene in Vmac ‘active’ gene
418 there is an additional anthocyanidin 3-O-galactosyltransferase that is fragmented and lacks the

419 complete active site, possibly explaining the dramatic differences in the anthocyanins between
420 the two species.

421

422 Several genes that may play key roles in pathogen resistance have been identified being under
423 selection pressure in the Vmac genomes. Both #35 and MQ show significant selection pressure
424 for *PGIP2*, believed to play an important role in resistance to microbial colonization [42]. *SMT1*,
425 a methyltransferase involved in sterol biosynthesis, is influential for innate immunity and the
426 formation of *FLS2* receptor kinase clustering (flagellin sensing 2) [43]. *HIR3* is part of the
427 hypersensitive response (HIR) gene family that has been shown to act in the defense of
428 microbial infection as well as influencing cellular response during viral infection [44]. *LYK4* (Lysin
429 motif domain receptor-like kinase 4) was shown to be an important plant defense component
430 against fungal infection and is a key signalling component in plant chitin response [45]. Other
431 genes found among the lines under selection pressure included *WRKY65*, *WRKY29*, *PALM1*,
432 and *MLO*. While these specific genes were found in both #35 and MQ, there are several unique
433 domains found in the wild relative Voxy that might offer further opportunity for incorporation into
434 agricultural varieties.

435

436 Interestingly we also found defense related genes under selection pressure to be differentially
437 expressed in the transcriptomes of other *Vaccinium* species during herbivory stress [46,47].
438 These genes included pleiotropic drug resistance transporter *ABCG36*, which provides
439 pathogen resistance in Arabidopsis [48,49] and *FAH1*, also identified to be an important
440 component of stress response in Arabidopsis [50]. Additionally, the serine/threonine-protein
441 kinase *D6PKL2*, part of the auxin response pathway, is upregulated during herbivory in chickpea
442 as well as bilberry [47,51]. In addition to pathogen resistance, several genes in the various
443 Vmac lines were identified under selection pressure for stress tolerance. One of the key
444 stressors includes drought stress, which is of particular importance to cultivated cranberry as a
445 large portion of time in dormancy is spent under drought conditions. These genes include *CIPK2*
446 [52], *AVP1* [53], *GAI* [54], *CPK20* [55], and *ABI4* [56]. Wax production on the fruit surface is an
447 important trait for the protection against pathogens, UV damage, and for limiting moisture loss.
448 We identified three genes that are related to wax production and UV protection that were under
449 selection pressure in the Vmac lines. These genes included *PALM1* [57], *KCS2* [58], both
450 relating to epicuticular wax production, and *MSH2* which is required for mitigation of UV-B light
451 damage [59].

452

453 Changes in circadian components could be pressured due to the latitudes at which Voxy and
454 Vmac reside. Ranges at higher latitudes could necessitate a greater amount of flexibility in the
455 core circadian oscillator to compensate for large swings in light dark cycles throughout the
456 course of the year. *LHY* is a key component of the core circadian oscillator, and *LHY* mutants
457 have shown to have short photoperiods [60], while *PRR9* is an important component in the
458 entrainment of the core oscillator to changes in photoperiod [61]. Taken together, changes in
459 these circadian components could have larger downstream effects on seasonal flowering and
460 fruit development [61–63].

461

462 Several other crop species have shown that circadian control and adaptation of photoperiod is
463 important for both domestication and augmentation of desired traits, including flowering time,
464 yield, and nutrient content [64–66]. The domestication of pea has been linked with variation in
465 circadian genes for photoperiod response, including *HR* and *ELF3* [67] , which are important
466 interaction partners of *LHY* and *PRR9* for the regulation of photoperiod response [68,69]. This
467 response allowed peas (*Pisum sativum*) to be cultivated at different latitudes, much like the
468 differences between wild Voxy and Vmac. Additionally, flowering time expression is altered in
469 domesticated cucumber when grown at varying latitudes [70]. Although we did not find the gene
470 *FT*, a major influencer of flowering time, to be different between Vmac and Voxy, *LHY* is a key
471 component in its regulation [62].
472

473 **Methods**

474 *Plant growth*

475 The cranberry cultivar Ben Lear (Vmac) was selected from the wild in Berlin, Wisconsin
476 (43.9680° N, 88.9434° W) in 1901 [10]. To reduce heterozygosity, a fifth-generation selfing cycle
477 inbred clone ($F \geq 0.97$) of ‘Ben Lear’ designated BL-S5 (accession CNJ95-125-1) was selected
478 for genome sequencing. The Voxy sequenced and used for hybridization with Vmac was
479 collected near Gakona, Alaska (62.3019° N, 145.3019° W) in 1996 and designated NJ96-20
480 [15]. The hybrid (Vmac X Voxy) was the result of a cross ('Stevens' x NJ96-20) made by N.
481 Vorsa in 1998, designated CNJ98-325-33. The ploidy of all cultivars and accessions used was
482 confirmed by flow cytometry [22]. All plants were maintained in 6 inch pots containing sandy soil
483 and fertilized with azalea mix for acidic plants. While maintained in a greenhouse, plants were
484 allowed to winter chill and developed as ambient temperature increased.
485

486 *DNA extraction*

487 Fresh leaf tissue of Vmac (CNJ95-125-1; BL-S5), Voxy (NJ96-20), and the hybrid (Vmac X
488 Voxy, CNJ98-325-33) was stored in the dark for 3 days to reduce the polysaccharides. Tissue
489 was then flash frozen in liquid nitrogen and ground into fine powder using mortar and pestle.
490 High molecular weight (HMW) DNA was extracted with a modified CTAB protocol, optimized for
491 cranberry [71]. HMW DNA was checked for quality on a Bioanalyzer (Agilent, Santa Clara, CA,
492 USA) and length on a standard agarose gel. HMW DNA was used for library construction and
493 sequencing on the long read Oxford Nanopore Technologies (ONT, Oxford, UK) platform and
494 the Illumina (San Diego, CA) short read platform.
495

496 *Sequencing*

497 HMW DNA was first sequenced on an ONT MinION sequencer to confirm quality for long read
498 Nanopore sequencing. Unsheared HMW DNA was used to make ONT ligation-based libraries.
499 Libraries were prepared starting with 1.5ug of DNA and following all other steps in ONT's
500 SQK-LSK109 protocol. Final libraries were loaded on an ONT flowcell (v9.4.1) and run on the
501 GridION. Bases were called in real-time on the GridION using the flip-flop version of Guppy
502 (v3.1). The resulting fastq files were concatenated (fail and pass) and used for downstream

503 genome assembly steps. Illumina 2x150 bp paired end reads were generated for genome size
504 estimates and polishing genome long read assemblies. Libraries for Illumina sequencing were
505 prepared from HMW DNA using NEBnext (NEB, Beverly, MA) and sequenced on the Illumina
506 NovaSeq (San Diego, CA). Illumina short reads for *V. macrocarpon* (CNJ95-125-1; BL-S5) were
507 accessed from NCBI (PRJNA245813).

508

509 *Genome size prediction by k-mer frequency*

510 Raw Illumina reads for *Vmac* (CNJ95-125-1; BL-S5; PRJNA245813), Voxy (NJ96-20) and the
511 hybrid (*Vmac* X *Voxy*) were analyzed for k-mer frequency (k=31) using Jellyfish (count -C -s 8G
512 -t 4 -m 31 and histo) [72]. Genome size was estimated and visualized using in house analysis
513 scripts as well as GenomeScope [21]. While *Vmac* and *Voxy* had single peaks consistent with
514 homozygous genomes, the hybrid had two peaks with the left peak bigger than the right peak,
515 consistent with tetraploidy or the fact that the two genomes are distinct (Table S1; Figure S2).

516

517 *Genome assembly*

518 Resulting ONT fastq files passing QC (fastq_pass) were assembled using our previously
519 described long read assembly pipeline [24]. Briefly, fastq files were filtered by length for the
520 longest 30x using a Illumina kmer-based genome size estimate [73]. The 30x fastq files were
521 overlapped using minimap2 [74], the initial assembly was generated with miniasm [75], the
522 resulting graph (gfa) was visually checked with Bandage [76], the assembly fasta was extracted
523 from the gfa (awk '/^S/{print ">"\$2"\n"\$3}' assembly_graph.gfa | fold >assembly_graph.fasta),
524 the consensus was generated with three (3) iterative cycles of mapping the 30x reads back to
525 the assembly with minimap2 followed by racon [77], and the final assembly was polished
526 iteratively three times (3) using 2x150 bp paired-end Illumina reads mapped using minimap2
527 (>98% mapping) followed by pilon [78]. The resulting assemblies were assessed for traditional
528 genome statistics including assessing genome completeness with Benchmarking Universal
529 Single-Copy Orthologs (BUSCO) (Table 1; Table S2) [79]. The genome graphs were visualized
530 using bandage (Figure 1) [76].

531

532 *Genome scaffolding*

533 Cranberry (*Vmac*) is closely related (i.e. it is in the same genus) to *V. corymbosum* (highbush
534 blueberry), which recently had an updated chromosome-scale genome release [25]. We
535 leveraged the haplotype-resolved blueberry genome to assess the quality of our *V.*
536 *macrocarpon* assembly by aligning our version 1 contig assembly (*Vmac_v1*) to haplotype 1 of
537 blueberry at both the DNA level and the protein level. *Vmac_v1* was aligned to *Vcor_hap1* using
538 minimap2 [74], and visualized the dotplot. *Vmac_v1* was also aligned to *V. corymbosum* at the
539 protein level using both CoGe [80], as well as MCscan
540 ([https://github.com/tanghaibao/jcvi/wiki/MCscan-\(Python-version\)](https://github.com/tanghaibao/jcvi/wiki/MCscan-(Python-version))) (Figure S3). Since the contig
541 contiguity (N50 length) was 15 Mb for the *Vmac_v1* assembly, which represents chromosome
542 arms, we leveraged the synteny with the chromosome resolved *Vcor_hap1* genome to orient
543 *Vmac_v1* contigs into super-scaffolds (chromosomes). The final *Vmac_v2* assembly revealed
544 several rearrangements between cranberry and blueberry, which were part of the original contig
545 structure of *Vmac_v1* (Figure S3). The *Vmac_v2* chromosome assembly was versified using a

546 high-density genetic map [26]. Linkage group (LG) specific anchors (>100 bp sequence) were
547 created from the previous genome assembly [19] and used to validate order and orientation of
548 Vmac_2 scaffolded contigs.

549

550 *Gene prediction and annotation*

551 Genomes were first masked for repeat sequence before predicting protein coding genes.
552 Repeat sequence was identified using the Extensive *de-novo* TE Annotator (EDTA) pipeline [31]
553 (Table S3). ONT derived cDNA reads were aligned to the reference using minimap2 and then
554 assembled into transcript models using Stringtie. We additionally leveraged two Illumina paired
555 end cDNA libraries from SRA (SRR9047913, SRR1282422) as part of gene predictions. The
556 soft masked genome was then used to predict protein coding genes using the funnannotate
557 pipeline (<https://funannotate.readthedocs.io/>) leveraging the long read based transcript models
558 and the illumina short read cDNA as empirical training data (Table 1). The resulting gene
559 predictions were annotated using the eggNOG mapper [81].

560

561 *Disease Resistance*

562 The complete CDS regions of Voxy and Vmac were analyzed through PRGdb's DRAGO 2 API
563 [35] to identify disease resistance motifs and further predict disease resistance gene
564 annotations.

565

566 *Pollen Staining*

567 Pollen stainability, with 1% lactophenol cotton blue stain, was employed to assess gamete
568 fertility in Vmac and Voxy and the hybrid F1 interspecific progeny. Pollen was dusted on a
569 microscope slide in a drop of stain and cover slipped. Pollen tetrads were observed at 400x
570 magnification as described [82]. Pollen was determined to be viable if stained. Tetrads (pollen in
571 *Vaccinium* spp. is shed with the 4 products of a pollen mother cell, as a tetrahedron). Tetrads
572 were scored for 5 possible tetrad classes; four, three, two, one, or zero stained (viable) pollen
573 grains.

574

575 *Gene family analysis*

576 Gene family analysis was performed across several closely related species as well as several
577 more distantly related species using OrthoFinder with default settings [83]. *Arabidopsis thaliana*
578 (Araport11), *Amborella trichopoda* (v1) and *Vitis vinifera* (grape; v2.1) were accessed on
579 Phytozome (<https://phytozome-next.jgi.doe.gov/>). The highbush blueberry (*Vaccinium*
580 *corymbosum*) genome was accessed from CoGe (id34364) [25]; the rhododendron
581 (*Rhododendron williamsianum*) genome was accessed from CoGe (id51210) [27], the
582 persimmon (*Diospyros oleifera*) genome was accessed from <http://persimmon.kazusa.or.jp> [28],
583 the tea (*Camellia sinensis*) genome was accessed from <http://tpia.teaplant.org> [29] and the kiwi
584 (*Actinidia chinensis*) genome was accessed from <ftp://bioinfo.bti.cornell.edu/pub/kiwifruit> [30].
585 Colored blocks in the figure generated (Fig. 2B) symbolize chromosomes or scaffolds while the
586 lines (grey) symbolize syntetic regions between genomes. The Upset plot was generated from
587 the orthogroup overlap file. The phylogenetic tree was constructed from the species_tree output
588 from Orthofinder [83].

589

590 *Whole genome duplication (WGD) analysis*

591 The genomes described in the gene family analysis were used for WGD analysis. Genomes for
592 *A. thaliana*, *A. trichopoda*, grape, blueberry, rhododendron, persimmon, tea, and kiwi were
593 aligned at the protein level using lastal in the MCscan python framework to calculate Ks and
594 identify percentage of syntenic blocks across the genome pairs
595 ([https://github.com/tanghaibao/jcvi/wiki/MCscan-\(Python-version\)](https://github.com/tanghaibao/jcvi/wiki/MCscan-(Python-version))). Similar calculations were
596 performed with genomes in CoGe [80] and FracBias was leveraged to confirm or identify
597 syntenic block numbers underlying WGD events [84]. Karyotype figures were generated using
598 MCscan python.

599

600 *Syntenic analysis*

601 Syntenic analysis was performed between Vmac and Voxy using SyMAP v5 [85]. Data from the
602 genome assembly as well as annotations of both genomes were imputed into SyMAP, though
603 contigs of size less than 100 kb were not analyzed, while the otherwise default parameters were
604 used to calculate synteny (-min_dots=7 -minScore=30 -minIdentity=70 - tileSize=10
605 -qMask=lower -maxIntron=10000). The subsequent analysis of overlapping syntenic blocks was
606 performed with python scripting, where concurrent genome blocks of Voxy that overlapped the
607 same location of Vmac were identified and gene annotation information of Voxy was pulled for
608 further review.

609

610 *KaKs pressure*

611 KaKs differences between Vmac and Voxy were calculated using gKaKs [86]. Genes under
612 selection pressure ($dN/dS > 1$) were cataloged for further analysis. GO terms were associated
613 with genes by cross referencing the annotated gene name and the available data in the Uniprot
614 database. Those GO terms associated with genes under selection pressure were collected for
615 comparison. In addition, we compared two cultivars that are considered early domesticated
616 varieties; Stevens (ST), #35, and a 3rd, later-domesticated variety Mullica Queen (MQ), with the
617 wild reference, Ben Lear (BL). We identified differential GO terms between wild and
618 domesticated lines, as well as several genes under selection pressure.

619

620 *Resequencing data analysis*

621 Multiple generations of the BL inbreeding lines, as well as parents from several other lines
622 important to the cranberry breeding program, were sequenced on the Illumina NGS platform.
623 These included 'Stevens', '#35', 'Mullica Queen', 'Ben Lear', a 5th generation self of 'Ben Lear'
624 (BL-S5), and a wild accession of Voxy. Pedigree information of the resequenced parental lines
625 can be found in [26]. Paired-end Illumina reads were aligned to the newly constructed Vmac
626 reference genome (Vmac-v2) using BWA-MEM [87]. Reads were sorted and duplicate reads
627 were removed from alignment files using samtools sort and rmdup respectively. SNPs were
628 identified using samtools mpileup and bcftools call [88].

629

630 Further analysis was performed to identify comparative regions of high and low SNP density
631 between lines. A script was generated in Python where heterozygous SNPs of each line, that

632 were unique in both SNP position and nucleotide change for a single individual, were placed
633 into 250,000 bp bins along the genome. The variant data from the genomes of Voxy as well as
634 the genomes of the Ben Lear inbred lines (BL-S1 to BL-S7) were not used to determine
635 uniqueness of SNPs compared to the rest of the Vmac lines since Voxy as well as the inbred
636 lines would show disproportionate amounts of unique and non-unique SNPs respectively.
637 Significant variation of unique SNP density was calculated through bootstrapping using the
638 average SNP data of four representative varieties (Stevens, #35, Mullica Queen, and Ben Lear).
639 1,000 iterations were performed, where the aforementioned pooled SNPs were randomly
640 assigned a bin, with the 95th percentile of bin maximums constituting the bounds of high SNP
641 density and conversely, the 5th percentile of bin minimums constituting the bounds for low SNP
642 density.

643

644 **Author contributions**

645 TPM, JP, and NV conceived the study. TPM, KC and BA sequenced the genomes. TPM, JK,
646 and NH analyzed data. JP, JK, and TPM wrote the paper.

647

648 **Data availability**

649 The genomes are available through CoGe under genome ID 60226 and 60227 for Vmac and
650 Voxy respectively. In addition, both genome assemblies with annotation can be found at the
651 Genome Database for Vaccinium (<https://www.vaccinium.org>); Vmac accession number
652 GDV21001 and Voxy accession number GDV21002. Assemblies and relevant read data can be
653 located in NCBI under BioProject PRJNA738865; Vmac accession number SAMN19762178.

654

655 **Acknowledgements**

656 We thank Shane Poplawski and Rachael Gominsky for DNA extraction and sequencing support.
657 This research was funded through the following agencies and groups: USDA-NIFA-AFRI Grant
658 2017-67013-26215, New Jersey Blueberry and Cranberry Research Council and The Cranberry
659 Institute. This work was supported by the Tang Genomics Fund to T.P.M.

660

661 **Supplemental Tables**

662 **Table S1. Cranberry genome size estimates by k-mer frequency.**

663

664 **Table S2. Cranberry genome assembly BUSCO scores.**

665

666 **Table S3. Cranberry repeat prediction.**

667

668 **Table S4. Details of genes under positive selection between Vmac and Voxy.**

669

670 **Table S5. Gene ontology (GO) terms for tandem duplicated (TD) genes.**

671

672 **Table S6. Gene ontology (GO) terms for tandem duplicated (TD) genes unique to Vmac
673 and Voxy.**

674

675 **Table S7. Disease resistant genes predicted by DRAGO2 in syntenic blocks between**
676 **Vmac and Voxy.**

677

678 **Table S8. Orthogroup (OG) overrepresented gene ontology (GO).**

679

680 **Table S9. High and low SNP region gene numbers for cranberry cultivars and inbred**
681 **series.**

682

683 **Table S10. Stevens (ST) all high SNP regions significant GO terms.**

684

685 **Table S11. #35 all high SNP regions significant GO terms.**

686

687 **Table S12. MQ all high SNP regions significant GO terms.**

688

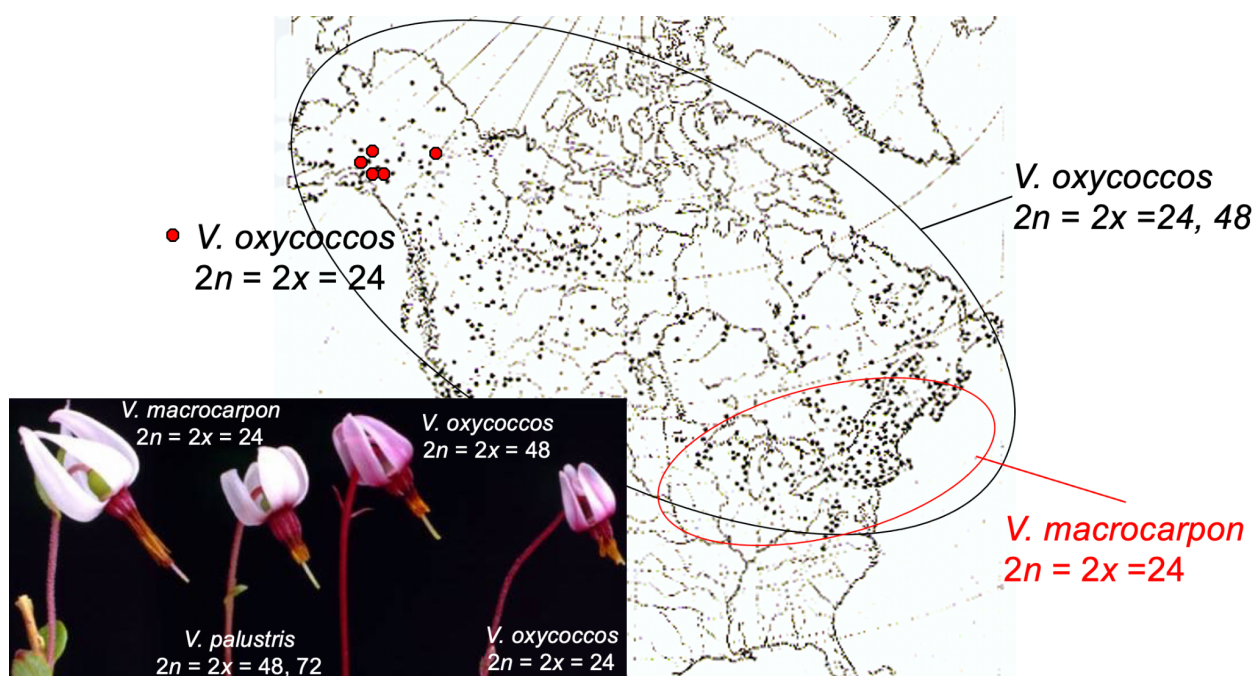
689 **Table S13. Genes under positive selection between important cranberry breeding**
690 **cultivars and the wild selection Ben Lear (BL).**

691

692

693 **Supplemental Figures**

694



695

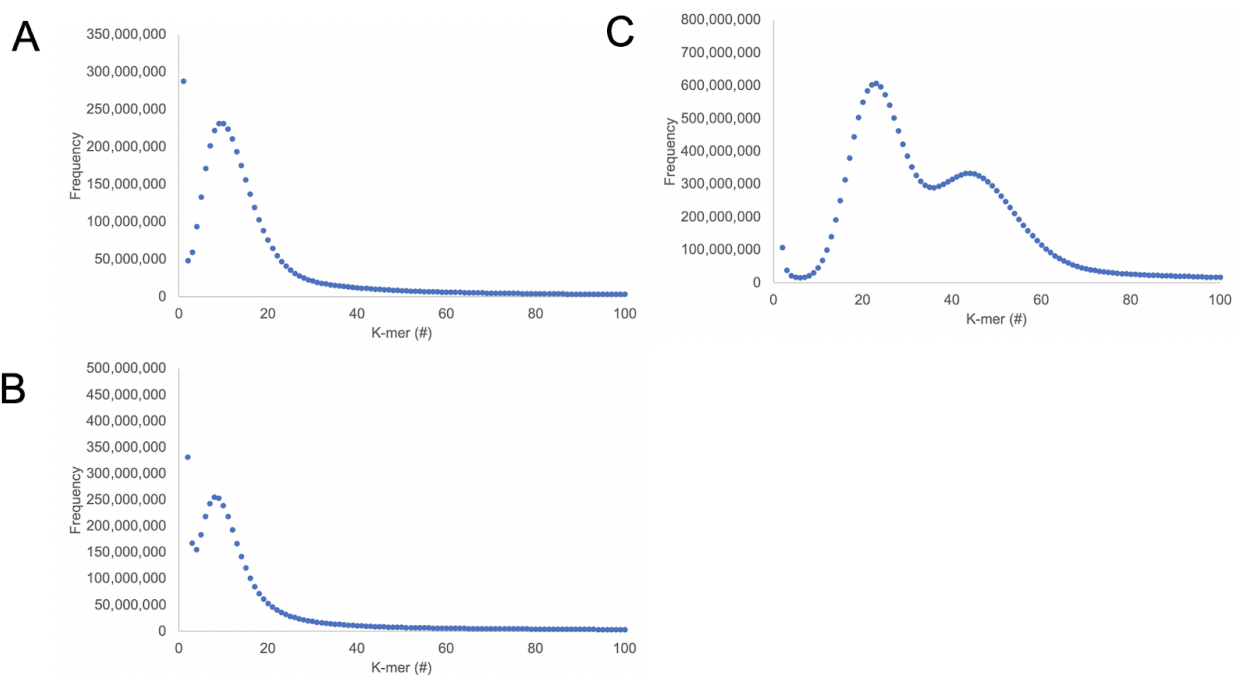
696 **Figure S1. *V. macrocarpon* and *V. oxycoccus* distribution and flower size comparison.**

697 Diploid *V. macrocarpon* is found in the Northeastern parts of the United States (US), while the
698 diploid *V. oxycoccus* is found in the Northwestern US and Canada.

699

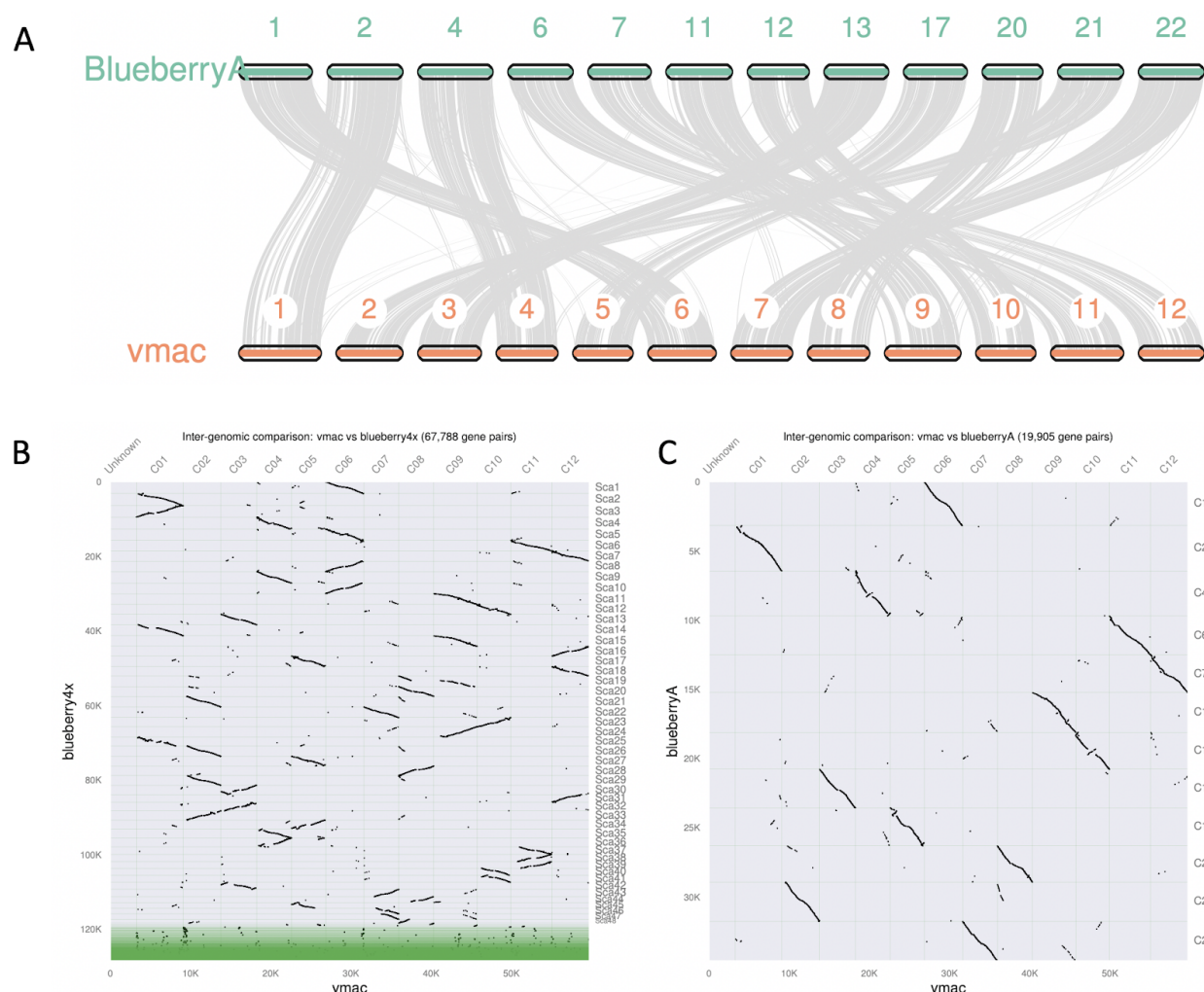
700

701

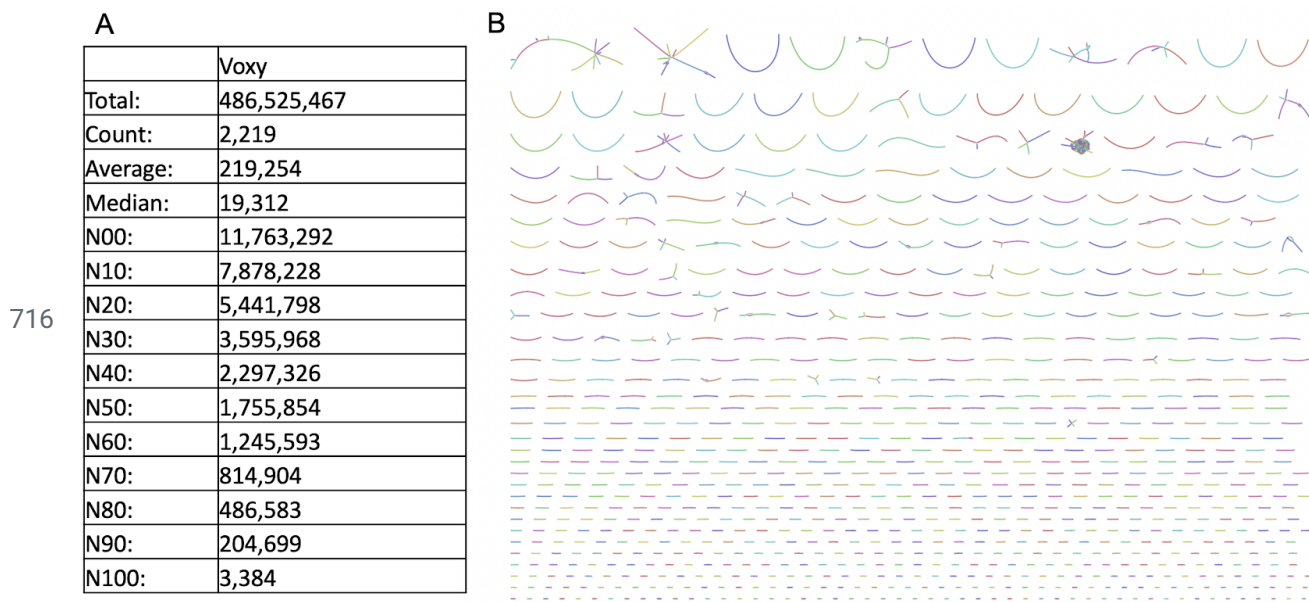


702

703 **Figure S2. *V. macrocarpon* and *V. oxycoccus* genomes size estimated by K-mer.** Genome
704 sizes were estimated by K-mer ($k=19$) frequency using Illumina paired short reads (2×150 bp)
705 for A) *V. macrocarpon* (Vmac), B) *V. oxycoccus* (Voxy), and C) the F1 hybrid. K-mers were
706 counted with Jellyfish and histogram was plotted to find the peak.
707

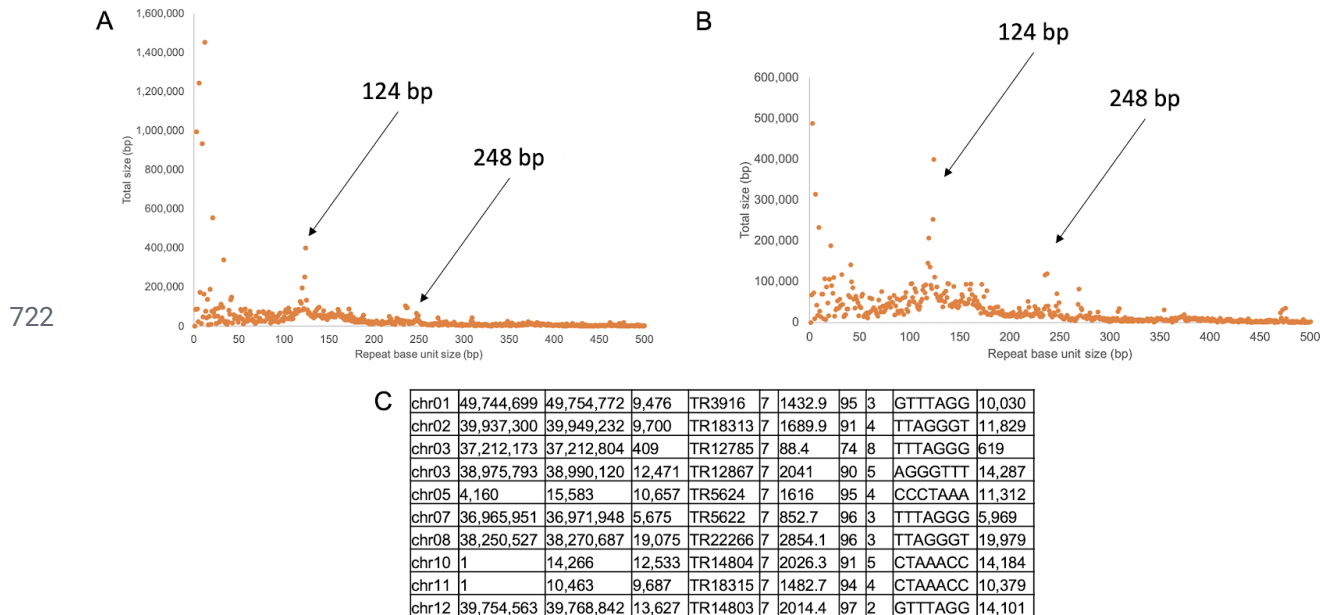


709 **Figure S3. The *V. macrocarpon* (Vmac) genome is highly syntenic with**
710 **chromosome-resolved blueberry (*V. corymbosum*) genome.** A) Blueberry haplotype A
711 (BlueberryA) was aligned to the Vmac assembly and are presented in the order of their
712 assigned chromosome numbers. B) Dot plot based on protein alignments between the
713 haplotype-resolved tetraploid blueberry (blueberry4x) and Vmac. C) Dot plot based on protein
714 alignments between the blueberry haplotype A (blueberryA) and Vmac.
715

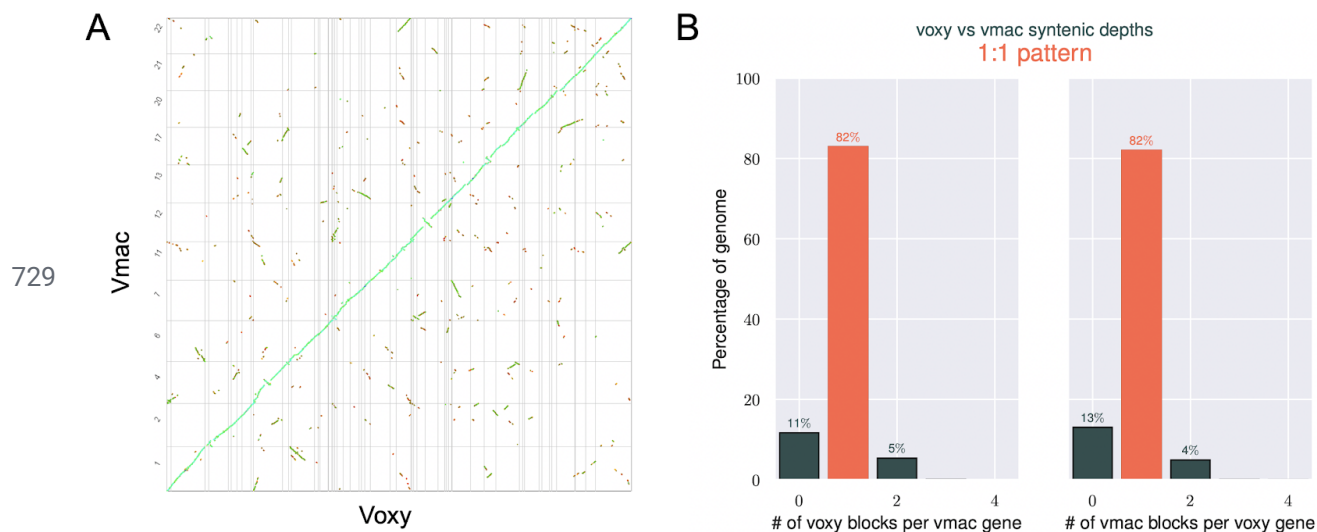


717 **Figure S4. *V. oxycoccus* (Voxy) contig assembly and graph.** A) Summary of the Voxy contig
718 assembly statistics. The Voxy assembly was 486 Mb, had a N50 length of 1.8 Mb, with the
719 longest contig being 11.8 Mb. B) The assembly graph of Voxy reveals low heterozygosity due to
720 the lack of extensive branching.

721

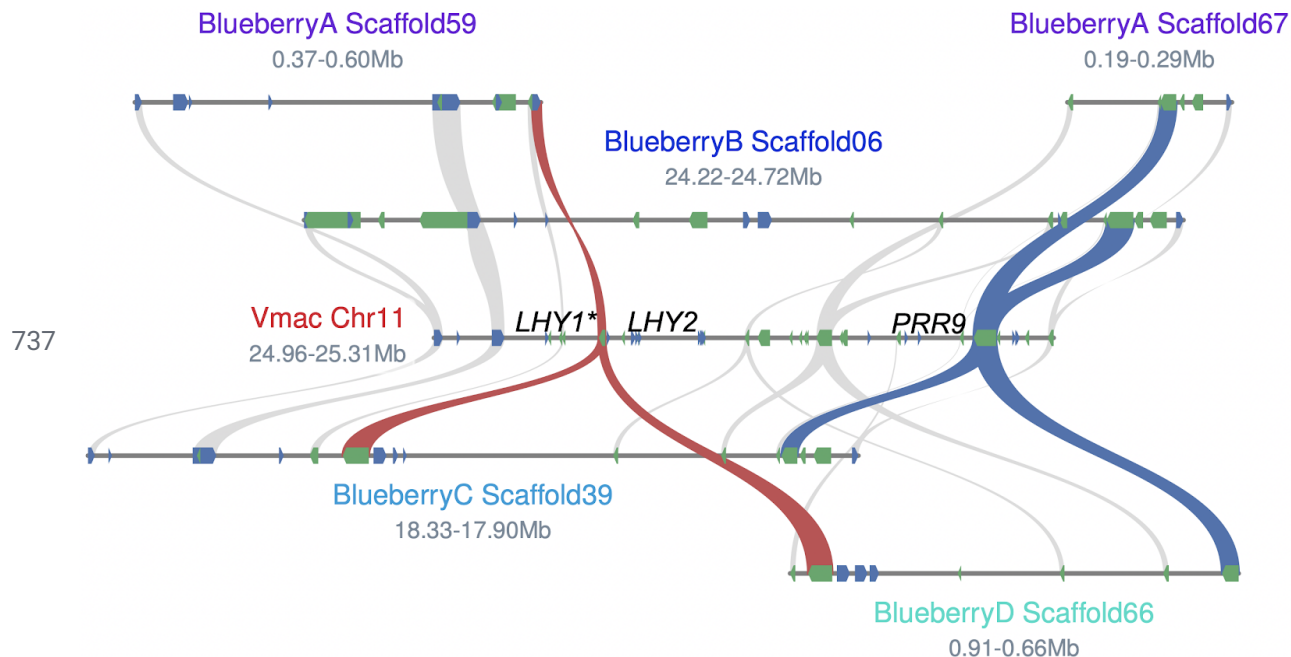


723 **Figure S5. *V. macrocarpon* (Vmac) centromere and telomere arrays.** A) Tandem repeats
724 were identified using Tandem Repeat Finder (TRF) and plotted by repeat unit size, which
725 revealed a 124 bp centromere base unit with a 248 bp higher repeat (HOR) consistent with a
726 centromere array. B) A similar centromere array with a base unit of 124 bp and HOR of 248 bp
727 was identified in Voxy. C) Telomere arrays with the 7 bp base unit (AAACCCCT) were identified in
728 the Vmac assembly, which revealed an average telomere length of 12 kb.



729 **Figure S6. *V. macrocarpon* (Vmac) and *V. oxycoccus* (Voxy) are highly collinear. A)** The
 730 Voxy scaffolds were aligned (protein) to the Vmac chromosomes revealing the two genomes are
 731 highly collinear with remnants of a recent whole genome duplication (WGD). Vertical and
 732 horizontal grey lines represent breaks in Chromosomes (Vmac) and scaffolds (Voxy) B)
 733 Syntenic depths between Vmac and Voxy suggest a 1:1 pattern, although there are remnants of
 734 a past WGD at 4-5%.

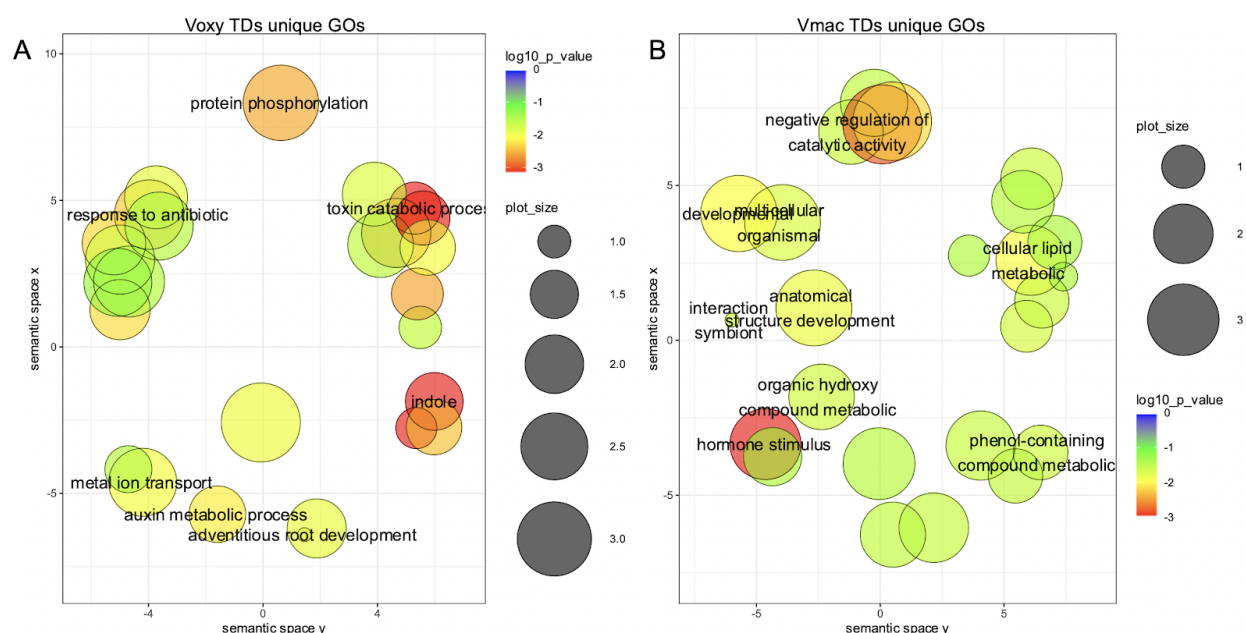
735



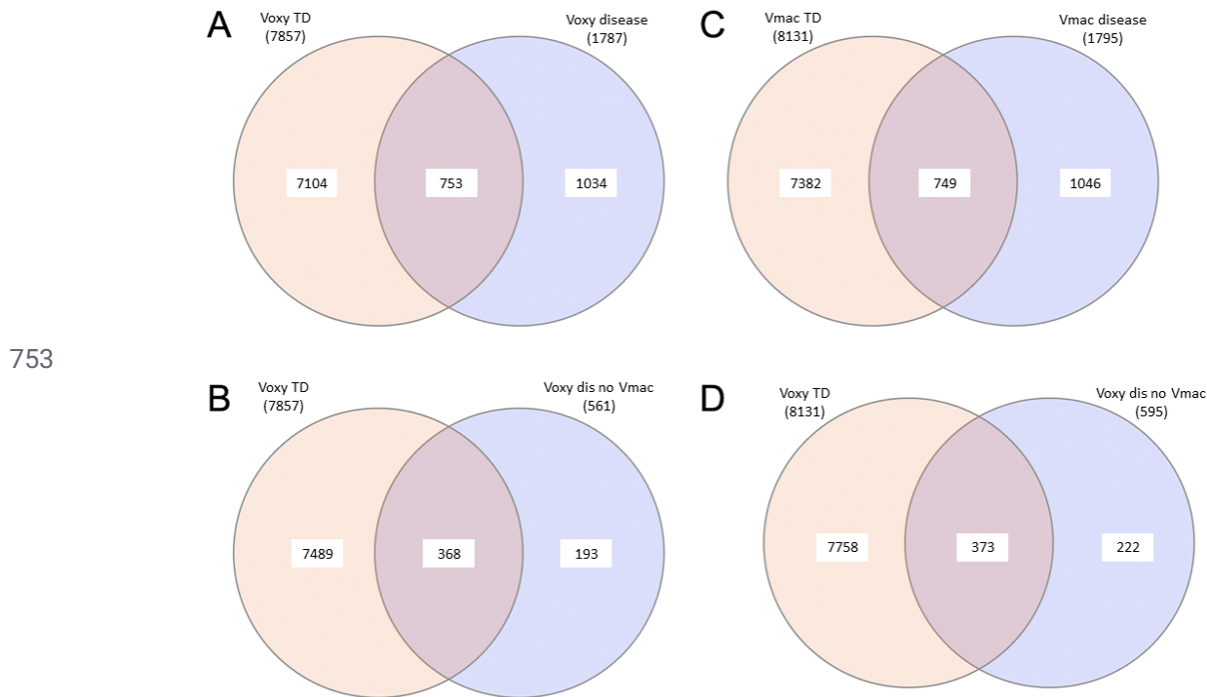
736
 737 **Figure S7. Tight linkage between core circadian clock genes is shared between cranberry**
and blueberry, but LHY tandem duplication (TD) is specific to cranberry. The
 738 haplotype-resolved blueberry genome was mapped to the Vmac genome to identify synteny
 739 blocks (grey lines). Blueberry has the core circadian clock linkage of *LHY* (red lines)-*PRR9* (blue
 740 lines) on three of its haplotypes, but it has been lost on haplotype B on Scaffold6. The *LHY*
 741

743 tandem duplication is specific to the Vmac lineage since it is not found in Voxy (Figure 2) nor
744 blueberry.
745

746



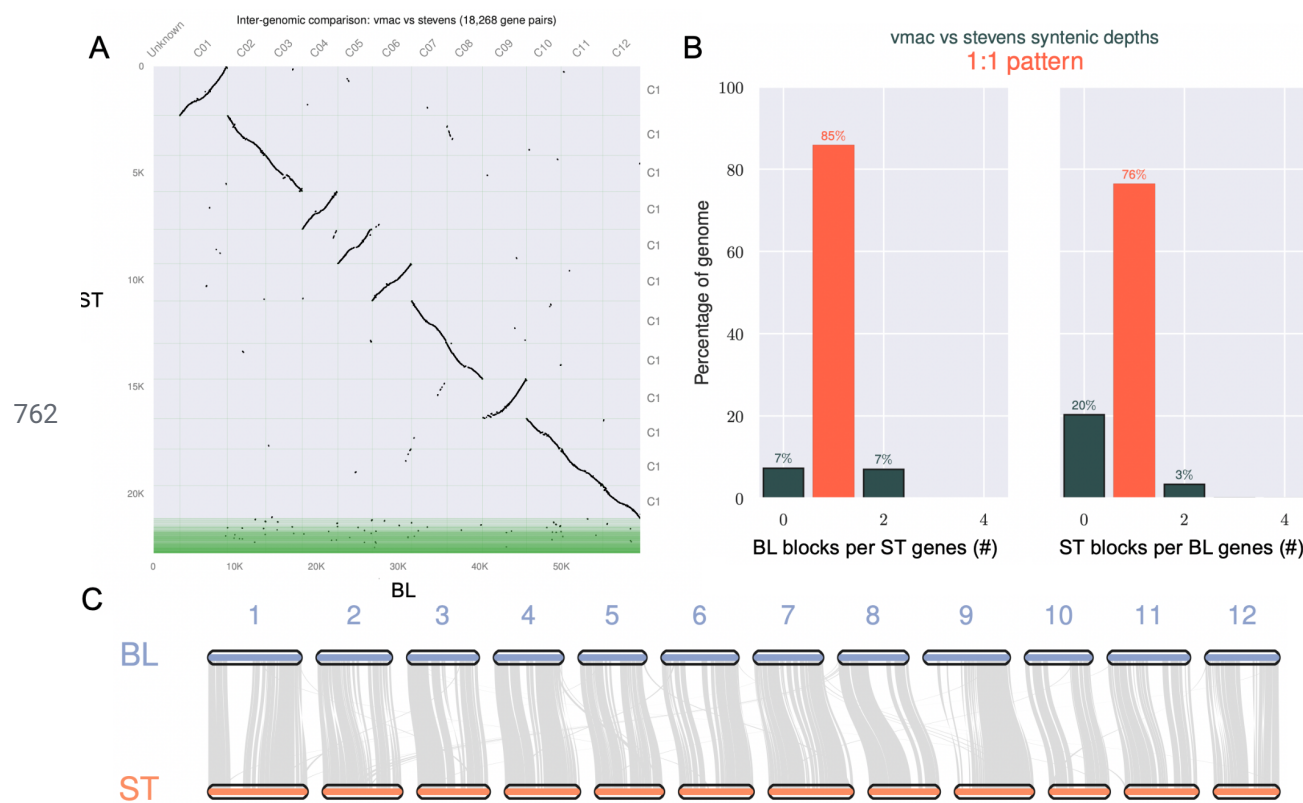
747 **Figure S8. Overrepresented gene ontology (GO) terms found in unique tandem
748 duplications (TDs) for *V. macrocarpon* (Vmac).** A) *V. oxycoccus* (Voxy) TDs unique GOs are
749 plotted in semantic space. B) Vmac TDs unique GOs are plotted in semantic space.
750 Significance is colored with red being the most significant and blue the least significant. The size
751 of the circle represents the number of elements.
752



753
754 **Figure S9. Venn diagrams of overlaps between predicted disease resistance genes and**
755 **tandem duplications (TDs) in the *V. oxyccoccus* (Voxy) and *V. macrocarpon* (Vmac)**
756 **genomes. A) Voxy TD overlaps with predicted disease resistance genes, and B) disease**
757 **resistance genes specific to Voxy (no syntenic ortholog in Vmac). C) Vmac TD overlaps with**
758 **predicted disease resistance genes, and D) disease resistance genes specific to Vmac (no**
759 **syntenic ortholog in Voxy).**

760

761



763 **Figure S10. Comparison of the inbred *V. macrocarpon* Ben Lear S5 (BL) and the recently**
764 **published Stevens (ST).** A) Dotplot between BL and ST based on protein-protein comparisons

765 reveals differences in chromosome size between the two access but high collinearity. Green

766 area for ST are the contigs not included in the chromosomes. B) Syntenic ortholog patterns

767 between BL and ST reveals that the ST genome is more fragmented than the BL genome due

768 to more (20% vs 7%) genes with zero (0) synteny blocks. C) Chromosome alignment between

769 BL and ST with grey lines representing synteny blocks. The missing regions between the two

770 assemblies are centromere and repeat regions missing in ST.

771

772 References

- 773 1. Vinson JA, Bose P, Proch J, Al Kharrat H, Samman N. Cranberries and cranberry products:
774 powerful in vitro, ex vivo, and in vivo sources of antioxidants. *J Agric Food Chem.* 2008;56:
775 5884–5891.
- 776 2. Wang Y, Singh AP, Nelson HN, Kaiser AJ, Reker NC, Hooks TL, et al. Urinary Clearance of
777 Cranberry Flavonol Glycosides in Humans. *J Agric Food Chem.* 2016;64: 7931–7939.
- 778 3. Feng G, Klein MI, Gregoire S, Singh AP, Vorsa N, Koo H. The specific
779 degree-of-polymerization of A-type proanthocyanidin oligomers impacts *Streptococcus*
780 mutans glucan-mediated adhesion and transcriptome responses within biofilms. *Biofouling.*
781 2013;29: 629–640.
- 782 4. Shabrova EV, Tarnopolsky O, Singh AP, Plutzky J, Vorsa N, Quadro L. Insights into the
783 molecular mechanisms of the anti-atherogenic actions of flavonoids in normal and obese

- 784 mice. PLoS One. 2011;6: e24634.
- 785 5. Wilson T, Meyers SL, Singh AP, Limburg PJ, Vorsa N. Favorable glycemic response of type
786 2 diabetics to low-calorie cranberry juice. J Food Sci. 2008;73: H241–5.
- 787 6. Koo H, Duarte S, Murata RM, Scott-Anne K, Gregoire S, Watson GE, et al. Influence of
788 cranberry proanthocyanidins on formation of biofilms by *Streptococcus mutans* on
789 saliva-coated apatitic surface and on dental caries development in vivo. Caries Res.
790 2010;44: 116–126.
- 791 7. USDA - national agricultural statistics service - publications - 2019 agricultural statistics
792 annual. [cited 14 Jan 2021]. Available:
793 https://www.nass.usda.gov/Publications/Ag_Statistics/2019/index.php
- 794 8. Food and Agriculture Organization of the United Nations. Agricultural production baselines
795 of key staple crops. United Nations Publications; 2018. doi:10.18356/4af814df-en
- 796 9. Read DJ. The Structure and Function of the Ericoid Mycorrhizal Root. Ann Bot. 1996;77:
797 365–374.
- 798 10. Eck P. The American Cranberry. Rutgers University Press; 1990.
- 799 11. Chandler FB, Demoranville IE. Rest period for cranberries. Proc Amer Soc Hort Sci. 1964.
800 pp. 307–311.
- 801 12. Eady FC, Eaton GW. Effects of chilling during dormancy on development of the terminal
802 bud of the cranberry. Can J Plant Sci. 1972;52: 273–279.
- 803 13. Vander Kloet SP. THE TAXONOMY OF VACCINIUM § OXYCOCCUS. Rhodora. 1983;85:
804 1–43.
- 805 14. Camp WH. A Preliminary Consideration of the Biosystematy of Oxycoccus. Bull Torrey Bot
806 Club. 1944;71: 426–437.
- 807 15. Mahy G, Bruederle LP, Connors B, Van Hofwegen M, Vorsa N. Allozyme evidence for
808 genetic autoployploidy and high genetic diversity in tetraploid cranberry, *Vaccinium*
809 *oxycoccus*(Ericaceae). American Journal of Botany. 2000. pp. 1882–1889.
810 doi:10.2307/2656840
- 811 16. Smith TW, Walinga C, Wang S, Kron P, Suda J, Zalapa J. Evaluating the relationship
812 between diploid and tetraploid *Vaccinium oxycoccus* (Ericaceae) in eastern Canada.
813 Botany. 2015;93: 623–636.
- 814 17. Bruederle LP, Hugan MS, Dignan JM, Vorsa N. Genetic Variation in Natural Populations of
815 the Large Cranberry, *Vaccinium macrocarpon* Ait. (Ericaceae). Bull Torrey Bot Club.
816 1996;123: 41–47.
- 817 18. Vorsa N, Polashock JJ. Alteration of anthocyanin glycosylation in cranberry through
818 interspecific hybridization. J Am Soc Hortic Sci. 2005;130: 711–715.
- 819 19. Polashock J, Zelzion E, Fajardo D, Zalapa J, Georgi L, Bhattacharya D, et al. The American

- 820 cranberry: first insights into the whole genome of a species adapted to bog habitat. BMC
821 Plant Biol. 2014;14: 165.
- 822 20. Diaz-Garcia L, Garcia-Ortega LF, González-Rodríguez M, Delaye L, Iorizzo M, Zalapa J.
823 Chromosome-Level Genome Assembly of the American Cranberry (*Vaccinium*
824 *macrocarpon* Ait.) and Its Wild Relative *Vaccinium microcarpum*. Front Plant Sci. 2021;12:
825 633310.
- 826 21. Vurtue GW, Sedlazeck FJ, Nattestad M, Underwood CJ, Fang H, Gurtowski J, et al.
827 GenomeScope: fast reference-free genome profiling from short reads. Bioinformatics.
828 2017;33: 2202–2204.
- 829 22. Zdepski A, Debnath SC, Howell A, Polashock J, Oudemans P, Vorsa N, et al. Cranberry.
830 Genetics, genomics and breeding of berries. CRC Press; 2016. pp. 41–63.
- 831 23. Michael TP, VanBuren R. Building near-complete plant genomes. Curr Opin Plant Biol.
832 2020;54: 26–33.
- 833 24. Michael TP, Jupe F, Bemm F, Motley ST, Sandoval JP, Lanz C, et al. High contiguity
834 *Arabidopsis thaliana* genome assembly with a single nanopore flow cell. Nat Commun.
835 2018;9: 541.
- 836 25. Colle M, Leisner CP, Wai CM, Ou S, Bird KA, Wang J, et al. Haplotype-phased genome and
837 evolution of phytonutrient pathways of tetraploid blueberry. Gigascience. 2019;8.
838 doi:10.1093/gigascience/giz012
- 839 26. Schlautman B, Covarrubias-Pazaran G, Diaz-Garcia L, Iorizzo M, Polashock J, Grygleski E,
840 et al. Construction of a High-Density American Cranberry (*Vaccinium macrocarpon* Ait.)
841 Composite Map Using Genotyping-by-Sequencing for Multi-pedigree Linkage Mapping. G3:
842 Genes|Genomes|Genetics. 2017. pp. 1177–1189. doi:10.1534/g3.116.037556
- 843 27. Soza VL, Lindsley D, Waalkes A, Ramage E, Patwardhan RP, Burton JN, et al. The
844 Rhododendron Genome and Chromosomal Organization Provide Insight into Shared
845 Whole-Genome Duplications across the Heath Family (Ericaceae). Genome Biol Evol.
846 2019;11: 3353–3371.
- 847 28. Suo Y, Sun P, Cheng H, Han W, Diao S, Li H, et al. A high-quality chromosomal genome
848 assembly of *Diospyros oleifera* Cheng. Gigascience. 2020;9.
849 doi:10.1093/gigascience/giz164
- 850 29. Zhang Q-J, Li W, Li K, Nan H, Shi C, Zhang Y, et al. SMRT sequencing yields the
851 chromosome-scale reference genome of tea tree, *Camellia sinensis* var. *sinensis*. 2020. p.
852 2020.01.02.892430. doi:10.1101/2020.01.02.892430
- 853 30. Wu H, Ma T, Kang M, Ai F, Zhang J, Dong G, et al. A high-quality *Actinidia chinensis*
854 (kiwifruit) genome. Hortic Res. 2019;6: 117.
- 855 31. Ou S, Su W, Liao Y, Chougule K, Ware D, Peterson T, et al. Benchmarking Transposable
856 Element Annotation Methods for Creation of a Streamlined, Comprehensive Pipeline.

- 857 doi:10.1101/657890
- 858 32. Choi JY, Abdulkina LR, Yin J, Chastukhina IB, Lovell JT, Agabekian IA, et al. Natural
859 variation in plant telomere length is associated with flowering time. *Plant Cell*. 2021.
860 doi:10.1093/plcell/koab022
- 861 33. Muroi A, Matsui K, Shimoda T, Kihara H, Ozawa R, Ishihara A, et al. Acquired immunity of
862 transgenic torenia plants overexpressing agmatine coumaroyltransferase to pathogens and
863 herbivore pests. *Sci Rep*. 2012;2: 689.
- 864 34. Mammadov J, Buyyarapu R, Guttikonda SK, Parliament K, Abdurakhmonov IY, Kumpatla
865 SP. Wild Relatives of Maize, Rice, Cotton, and Soybean: Treasure Troves for Tolerance to
866 Biotic and Abiotic Stresses. *Front Plant Sci*. 2018;9: 886.
- 867 35. Osuna-Cruz CM, Paytuvi-Gallart A, Di Donato A, Sundesha V, Andolfo G, Aiese Cigliano R,
868 et al. PRGdb 3.0: a comprehensive platform for prediction and analysis of plant disease
869 resistance genes. *Nucleic Acids Res*. 2018;46: D1197–D1201.
- 870 36. Fong SK, Kawash J, Wang Y, Johnson-Cicalese J, Polashock J, Vorsa N. A low malic acid
871 trait in cranberry fruit: genetics, molecular mapping, and interaction with a citric acid locus.
872 *Tree Genet Genomes*. 2021;17: 4.
- 873 37. Akagi T, Shirasawa K, Nagasaki H, Hirakawa H, Tao R, Comai L, et al. The persimmon
874 genome reveals clues to the evolution of a lineage-specific sex determination system in
875 plants. *PLoS Genet*. 2020;16: e1008566.
- 876 38. Huang S, Ding J, Deng D, Tang W, Sun H, Liu D, et al. Draft genome of the kiwifruit
877 *Actinidia chinensis*. *Nat Commun*. 2013;4: 2640.
- 878 39. Steed G, Ramirez DC, Hannah MA, Webb AAR. Chronoculture, harnessing the circadian
879 clock to improve crop yield and sustainability. *Science*. 2021;372.
880 doi:10.1126/science.abc9141
- 881 40. Vogt T, Jones P. Glycosyltransferases in plant natural product synthesis: characterization of
882 a supergene family. *Trends Plant Sci*. 2000;5: 380–386.
- 883 41. Xu Z-S, Ma J, Wang F, Ma H-Y, Wang Q-X, Xiong A-S. Identification and characterization of
884 DcUCGALT1, a galactosyltransferase responsible for anthocyanin galactosylation in purple
885 carrot (*Daucus carota* L.) taproots. *Sci Rep*. 2016;6: 27356.
- 886 42. Kalunke RM, Tundo S, Benedetti M, Cervone F, De Lorenzo G, D’Ovidio R. An update on
887 polygalacturonase-inhibiting protein (PGIP), a leucine-rich repeat protein that protects crop
888 plants against pathogens. *Front Plant Sci*. 2015;6: 146.
- 889 43. Cui Y, Li X, Yu M, Li R, Fan L, Zhu Y, et al. Sterols regulate endocytic pathways during
890 flg22-induced defense responses in *Arabidopsis*. *Development*. 2018;145.
891 doi:10.1242/dev.165688
- 892 44. Li S, Zhao J, Zhai Y, Yuan Q, Zhang H, Wu X, et al. The hypersensitive induced reaction 3
893 (HIR3) gene contributes to plant basal resistance via an EDS1 and salicylic acid-dependent

- 894 pathway. *Plant J.* 2019;98: 783–797.
- 895 45. Wan J, Tanaka K, Zhang X-C, Son GH, Brechenmacher L, Nguyen THN, et al. LYK4, a
896 lysin motif receptor-like kinase, is important for chitin signaling and plant innate immunity in
897 *Arabidopsis*. *Plant Physiol.* 2012;160: 396–406.
- 898 46. Rodriguez-Saona CR, Polashock J, Malo EA. Jasmonate-Mediated Induced Volatiles in the
899 American Cranberry, *Vaccinium macrocarpon*: From Gene Expression to Organismal
900 Interactions. *Front Plant Sci.* 2013;4: 115.
- 901 47. Benevenuto RF, Seldal T, Hegland SJ, Rodriguez-Saona C, Kawash J, Polashock J.
902 Transcriptional profiling of methyl jasmonate-induced defense responses in bilberry
903 (*Vaccinium myrtillus* L.). *BMC Plant Biology.* 2019. doi:10.1186/s12870-019-1650-0
- 904 48. Bienert MD, Siegmund SEG, Drozak A, Trombik T, Bultreys A, Baldwin IT, et al. A
905 pleiotropic drug resistance transporter in *Nicotiana tabacum* is involved in defense against
906 the herbivore *Manduca sexta*. *Plant J.* 2012;72: 745–757.
- 907 49. Stein M, Dittgen J, Sánchez-Rodríguez C, Hou B-H, Molina A, Schulze-Lefert P, et al.
908 *Arabidopsis PEN3/PDR8*, an ATP binding cassette transporter, contributes to nonhost
909 resistance to inappropriate pathogens that enter by direct penetration. *Plant Cell.* 2006;18:
910 731–746.
- 911 50. Huby E, Napier JA, Baillieul F, Michaelson LV, Dhondt-Cordelier S. Sphingolipids: towards
912 an integrated view of metabolism during the plant stress response. *New Phytol.* 2020;225:
913 659–670.
- 914 51. Bhattacharjee M, Dhar S, Handique PJ, Acharjee S, Sarmah BK. Defense Response in
915 Chickpea Pod Wall due to Simulated Herbivory Unfolds Differential Proteome Profile.
916 *Protein J.* 2020;39: 240–257.
- 917 52. Wang Y, Sun T, Li T, Wang M, Yang G, He G. A CBL-Interacting Protein Kinase TaCIPK2
918 Confers Drought Tolerance in Transgenic Tobacco Plants through Regulating the Stomatal
919 Movement. *PLoS One.* 2016;11: e0167962.
- 920 53. Esmaeili N, Yang X, Cai Y, Sun L, Zhu X, Shen G, et al. Co-overexpression of AVP1 and
921 OsSIZ1 in *Arabidopsis* substantially enhances plant tolerance to drought, salt, and heat
922 stresses. *Scientific Reports.* 2019. doi:10.1038/s41598-019-44062-0
- 923 54. Wang Z, Liu L, Cheng C, Ren Z, Xu S, Li X. GAI Functions in the Plant Response to
924 Dehydration Stress in *Arabidopsis thaliana*. *Int J Mol Sci.* 2020;21.
925 doi:10.3390/ijms21030819
- 926 55. Dubrovina AS, Kiselev KV, Khristenko VS, Aleynova OA. VaCPK20 , a calcium-dependent
927 protein kinase gene of wild grapevine *Vitis amurensis* Rupr., mediates cold and drought
928 stress tolerance. *Journal of Plant Physiology.* 2015. pp. 1–12.
929 doi:10.1016/j.jplph.2015.05.020
- 930 56. Khan IU, Ali A, Khan HA, Baek D, Park J, Lim CJ, et al. PWR/HDA9/ABI4 Complex
931 Epigenetically Regulates ABA Dependent Drought Stress Tolerance in *Arabidopsis*. *Front*

- 932 57. Uppalapati SR, Ishiga Y, Doraiswamy V, Bedair M, Mittal S, Chen J, et al. Loss of Abaxial
933 Leaf Epicuticular Wax in *Medicago truncatula* *irg1/palm1* Mutants Results in Reduced
934 Spore Differentiation of Anthracnose and Nonhost Rust Pathogens. *The Plant Cell*. 2012.
935 pp. 353–370. doi:10.1105/tpc.111.093104
- 936 58. Lee S-B, Jung S-J, Go Y-S, Kim H-U, Kim J-K, Cho H-J, et al. Two *Arabidopsis* 3-ketoacyl
937 CoA synthase genes, KCS20 and KCS2/DAISY, are functionally redundant in cuticular wax
938 and root suberin biosynthesis, but differentially controlled by osmotic stress. *The Plant
939 Journal*. 2009. pp. 462–475. doi:10.1111/j.1365-313x.2009.03973.x
- 940 59. Lario LD, Ramirez-Parra E, Gutierrez C, Casati P, Spampinato CP. Regulation of plant
941 MSH2 and MSH6 genes in the UV-B-induced DNA damage response. *J Exp Bot*. 2011;62:
942 2925–2937.
- 943 60. Alabadí D, Yanovsky MJ, Más P, Harmer SL, Kay SA. Critical Role for CCA1 and LHY in
944 Maintaining Circadian Rhythmicity in *Arabidopsis*. *Curr Biol*. 2002;12: 757–761.
- 945 61. Nakamichi N, Kita M, Ito S, Yamashino T, Mizuno T. PSEUDO-RESPONSE REGULATORS,
946 PRR9, PRR7 and PRR5, together play essential roles close to the circadian clock of
947 *Arabidopsis thaliana*. *Plant Cell Physiol*. 2005;46: 686–698.
- 948 62. Park M-J, Kwon Y-J, Gil K-E, Park C-M. LATE ELONGATED HYPOCOTYL regulates
949 photoperiodic flowering via the circadian clock in *Arabidopsis*. *BMC Plant Biol*. 2016;16:
950 114.
- 951 63. Mockler T, Yang H, Yu X, Parikh D, Cheng Y-C, Dolan S, et al. Regulation of photoperiodic
952 flowering by *Arabidopsis* photoreceptors. *Proc Natl Acad Sci U S A*. 2003;100: 2140–2145.
- 953 64. Blümel M, Dally N, Jung C. Flowering time regulation in crops — what did we learn from
954 *Arabidopsis*? *Current Opinion in Biotechnology*. 2015. pp. 121–129.
955 doi:10.1016/j.copbio.2014.11.023
- 956 65. Bendix C, Marshall CM, Harmon FG. Circadian Clock Genes Universally Control Key
957 Agricultural Traits. *Mol Plant*. 2015;8: 1135–1152.
- 958 66. Müller NA, Wijnen CL, Srinivasan A, Ryngajlo M, Ofner I, Lin T, et al. Domestication
959 selected for deceleration of the circadian clock in cultivated tomato. *Nat Genet*. 2016;48:
960 89–93.
- 961 67. Weller JL, Liew LC, Hecht VFG, Rajandran V, Laurie RE, Ridge S, et al. A conserved
962 molecular basis for photoperiod adaptation in two temperate legumes. *Proc Natl Acad Sci U
963 S A*. 2012;109: 21158–21163.
- 964 68. Song H-R. Interaction between the Late Elongated hypocotyl (LHY) and Early flowering 3
965 (ELF3) genes in the *Arabidopsis* circadian clock. *Genes & Genomics*. 2012. pp. 329–337.
966 doi:10.1007/s13258-012-0011-2
- 967 69. Anwer MU, Boikoglou E, Herrero E, Hallstein M, Davis AM, James GV, et al. Natural

- 969 variation reveals that intracellular distribution of ELF3 protein is associated with function in
970 the circadian clock. *eLife*. 2014. doi:10.7554/elife.02206
- 971 70. Wang S, Li H, Li Y, Li Z, Qi J, Lin T, et al. FLOWERING LOCUS T Improves Cucumber
972 Adaptation to Higher Latitudes. *Plant Physiol*. 2020;182: 908–918.
- 973 71. Lutz KA, Wang W, Zdepski A, Michael TP. Isolation and analysis of high quality nuclear
974 DNA with reduced organellar DNA for plant genome sequencing and resequencing. *BMC*
975 *Biotechnol*. 2011;11: 54.
- 976 72. Marçais G, Kingsford C. A fast, lock-free approach for efficient parallel counting of
977 occurrences of k-mers. *Bioinformatics*. 2011;27: 764–770.
- 978 73. Li H. seqtk Toolkit for processing sequences in FASTA/Q formats. GitHub; 2012.
- 979 74. Li H. Minimap2: pairwise alignment for nucleotide sequences. *Bioinformatics*. 2018;34:
980 3094–3100.
- 981 75. Li H. Minimap and miniasm: fast mapping and de novo assembly for noisy long sequences.
982 *Bioinformatics*. 2016;32: 2103–2110.
- 983 76. Wick RR, Schultz MB, Zobel J, Holt KE. Bandage: interactive visualization of de novo
984 genome assemblies. *Bioinformatics*. 2015;31: 3350–3352.
- 985 77. Vaser R, Sović I, Nagarajan N, Šikić M. Fast and accurate de novo genome assembly from
986 long uncorrected reads. *Genome Res*. 2017;27: 737–746.
- 987 78. Walker BJ, Abeel T, Shea T, Priest M, Abouelliel A, Sakthikumar S, et al. Pilon: an
988 integrated tool for comprehensive microbial variant detection and genome assembly
989 improvement. *PLoS One*. 2014;9: e112963.
- 990 79. Simão FA, Waterhouse RM, Ioannidis P, Kriventseva EV, Zdobnov EM. BUSCO: assessing
991 genome assembly and annotation completeness with single-copy orthologs. *Bioinformatics*.
992 2015;31: 3210–3212.
- 993 80. Grover JW, Bomhoff M, Davey S, Gregory BD, Mosher RA, Lyons E. CoGe LoadExp+: A
994 web-based suite that integrates next-generation sequencing data analysis workflows and
995 visualization. *Plant Direct*. 2017;1. doi:10.1002/pld3.8
- 996 81. Huerta-Cepas J, Szklarczyk D, Heller D, Hernández-Plaza A, Forslund SK, Cook H, et al.
997 eggNOG 5.0: a hierarchical, functionally and phylogenetically annotated orthology resource
998 based on 5090 organisms and 2502 viruses. *Nucleic Acids Res*. 2019;47: D309–D314.
- 999 82. Ortiz R, Vorsa N. Tetrad Analysis with Translocation Heterozygotes in Cranberry (*Vaccinium*
1000 *Macrocarpon* Ait.): Interstitial Chiasma and Directed Segregation of Centromeres.
1001 *Hereditas*. 2004;129: 75–84.
- 1002 83. Emms DM, Kelly S. OrthoFinder: solving fundamental biases in whole genome
1003 comparisons dramatically improves orthogroup inference accuracy. *Genome Biol*. 2015;16:
1004 157.

- 1005 84. Joyce BL, Haug-Batzell A, Davey S, Bomhoff M, Schnable JC, Lyons E. FractBias: a
1006 graphical tool for assessing fractionation bias following polyploidy. *Bioinformatics*. 2017;33:
1007 552–554.
- 1008 85. Soderlund C, Bomhoff M, Nelson WM. SyMAP v3.4: a turnkey synteny system with
1009 application to plant genomes. *Nucleic Acids Res.* 2011;39: e68.
- 1010 86. Yang Z, Nielsen R. Estimating Synonymous and Nonsynonymous Substitution Rates Under
1011 Realistic Evolutionary Models. *Molecular Biology and Evolution*. 2000. pp. 32–43.
1012 doi:10.1093/oxfordjournals.molbev.a026236
- 1013 87. Li H. Aligning sequence reads, clone sequences and assembly contigs with BWA-MEM.
1014 arXiv [q-bio.GN]. 2013. Available: <http://arxiv.org/abs/1303.3997>
- 1015 88. Danecek P, Bonfield JK, Liddle J, Marshall J, Ohan V, Pollard MO, et al. Twelve years of
1016 SAMtools and BCFtools. *Gigascience*. 2021;10. doi:10.1093/gigascience/giab008
- 1017